

Journal of Climate

Interannual coupling between summertime surface temperature and precipitation over land: processes and implications for climate change --Manuscript Draft--

Manuscript Number:	JCLI-D-14-00324
Full Title:	Interannual coupling between summertime surface temperature and precipitation over land: processes and implications for climate change
Article Type:	Article
Corresponding Author:	Alexis Berg Rutgers, The State University of New Jersey New Brunswick, New jersey UNITED STATES
Corresponding Author's Institution:	Rutgers, The State University of New Jersey
First Author:	Alexis Berg
Order of Authors:	Alexis Berg Benjamin Lintner Kirsten Findell Sonia I. Seneviratne Bart van den Hurk Agnès Ducharne Frédérique Chéruy Stefan Hagemann David Lawrence Sergey Malyshev Arndt Meier Pierre Gentine
Abstract:	<p>Widespread negative correlations between summertime-mean temperatures and precipitation over land regions are a well-known feature of terrestrial climate. This behavior has generally been interpreted in the context of soil moisture-atmosphere coupling, with soil moisture deficits associated with reduced rainfall leading to enhanced surface sensible heating and higher surface temperature. The present study revisits the genesis of these negative temperature-precipitation correlations using simulations from the Global Land-Atmosphere Coupling Experiment - Coupled Model Intercomparison Project phase 5 (GLACE-CMIP5) multi-model experiment. The analyses are based on simulations with 5 climate models, which were integrated with prescribed (non-interactive) and with interactive soil moisture over the period 1950-2100. While the results presented here generally confirm the interpretation that negative correlations between seasonal temperature and precipitation arise through the direct control of soil moisture on surface heat flux partitioning, the presence of widespread negative correlations when soil moisture-atmosphere interactions are artificially removed in at least two out of five models suggests that atmospheric processes, in addition to land surface processes, contribute to the observed negative temperature-precipitation correlation. On longer timescales, the negative correlation between precipitation and temperature is shown to have implications for the projection of climate change impacts on near surface climate: in all models, in the regions of strongest temperature-precipitation anti-correlation on interannual timescales, long-term regional warming is modulated to a large extent by the regional response of precipitation to climate change, with precipitation increases (decreases) being associated with minimum (maximum) warming. This correspondence appears to arise largely as the result of soil-moisture atmosphere interactions.</p>

We thank the reviewers for their comments on the manuscript. Below are our answers to the comments.

Please note that the manuscript has been reorganized, figures added or removed, their order changed. For the sake of consistency with the reviewers' comments, unless otherwise stated references to figure or section number in our reply below refer to the initial version of the manuscript.

The main changes brought to the manuscript are as follows:

- The manuscript was reorganized (section 4, figures order) and the steps of the analysis clarified to account for reviewer #1's comment on the perceived redundancy of the analysis in our initial manuscript;
- Following reviewer #3's recommendation, temperature-precipitation correlations from observations were added to the analysis;
- Following reviewer #1 and #3 comments, all figures were reworked; correlation maps use a different color scale emphasizing statistical significance, and where non-significant values are not shown. The field significance of temperature-precipitation correlations was assessed.

Reflecting these changes, the text has been modified extensively throughout the manuscript.

Also, note that observations of T-P correlations added to the study were found to be sensitive to linear detrending. Because the focus was on interannual variability, we show linearly detrended results. For the sake of consistency, all model results are then presented detrended as well in the revised manuscript. Small quantitative differences with the initial results thus exist, however the main results of the analysis remain qualitatively unaffected.

Please note that we also clarified the title of the manuscript, adding "over land".

#####

Reviewer Comments included in this letter:

Reviewer #1: The authors provide an analysis of long term climate simulations that isolate the mechanisms underlying precipitation-temperature correlations. The paper is well-written, and I don't have any real problem with the science. The paper, though, is much longer than it needs to be (comment #1), which detracts from its usefulness. I recommend publication subject to minor revision, though the length issue may, in some ways, suggest major revision.

1. The main result of the paper is that over much of the world, low (high) precipitation rates lead to low (high) evaporation rates which in turn lead to high (low) temperatures, while a secondary mechanism (cloudiness associated with both increased precipitation and reduced incident radiation) can also be important in some situations. That's fine, and the multi-model demonstration of this seems worthy of documentation. However, this result is effectively presented several times, through different methods of processing the same data (map comparisons, histograms, binning, examination of temperature/evaporation correlations, examination of radiation/precipitation correlations, etc.). The reader will be convinced very early on of the paper's main result and doesn't particularly benefit from seeing the same result pop out of additional processing methods. Personally, I didn't learn much of anything from Figures 3-8 that wasn't already demonstrated or implied reasonably well in Figure 2.

Should the authors get rid of Figures 3-8? Maybe not all of them. Figure 3 is a nice summary and doesn't take up much room. Figures 4 and 5 show some potentially useful supporting information but do take up a lot of room; could multi-model averages be shown instead, given that model differences are not emphasized here, except for a few asides? As for Figures 6-7, I'll admit that they don't do anything for me. It's an interesting way to look at the data, but the information content is essentially the same as that of the earlier figures, so the reader has to do a lot of work for little gain. Figure 8 provides more supporting data, but again, the main findings were already presented, and I'm not fully convinced that the supporting data is needed.

While we agree with the reviewer's comment that Figure 2 already neatly contained the main results of the study, we still think figures 3-8 add value to the analysis and are actually necessary to explain the results in figure 2. We take the reviewer's comment here as showing that we failed to clearly define and separate the different parts of the analysis and their respective contributions:

- Figure 2 shows negative T-P correlations are reduced in all models from REF to expA, but subsist significantly in some models. Our *a priori* interpretation of Figure 2 is that soil moisture-atmosphere interactions have been disabled in expA by the suppression of interactive soil moisture, so that, while all processes represented on Figure 1 are active in REF and can contribute to simulated T-P covariability, only atmospheric processes play a role in these correlations in expA.
- Figure 4-5 confirm that in expA, the land only responds to the atmosphere (does not feed back to it) and Figure 8 provides some confirmation that in that context, negative T-P correlations in 1A seem to result from precipitation-radiation-temperature relationships (consistently with Figure 1).

- Figure 6-7 provide a separate but consistent line of analysis: the models that displayed negative T-P correlation in expA are also the ones that in simulation RF also display negative T-P correlations in regions of energy-limited evaporative regimes (in addition to displaying such correlations in soil moisture-limited regions); i.e., in both cases, they do so without soil moisture's feedbacks to the atmosphere. We feel this physical consistency between both simulations is worth presenting, as it reinforces the diagnosis of differences in model behavior. As a result we respectfully disagree with the reviewer's suggestion to remove Figure 6-7 and the corresponding analysis.

In response to the reviewer's comment, we have revised the manuscript to better separate the different stages of the analysis in the text and better underscore their respective contributions –e.g., lines 233-241, 294-299, 385-392 in the new manuscript. We also reorganized section 4 so that the text now follows the general plan outlined above, which we believe will be clearer than the initial version (that is, figures 4-5-6-7-8 have been rearranged as 4-5-8-6). To reduce the length of the manuscript, (former) Figure 7 was changed to Supplementary Material, as it helps understand Figure 6 but is not essential to the analysis. Note that Figure 3 now only shows Figure 3d, as surface areas of negative or positive correlations are now already shown on (former) Figure 2. We did consider showing multi-model averages for figures 4 and 5, but since these figures correspond to the axes on the binned plots on Figure 6, we think it is important to show them separately for each model to facilitate the understanding of Figure 6.

2. In any case, all of the figures need to be reworked. The caption in Figure 2, for example, says that blue and red contours indicate significance levels of 5%, but there are different shades of blue and red shown, so it's very difficult to interpret significance. The only approach that really makes sense here (in all the figures) is to mask out (i.e., plot as white) the values that are not significant at the 5% level.

The captions in the initial manuscript referred to the blue and red contour, *i.e. contour lines*, that showed 5% significance – not to the shading. We are sorry if that was unclear. In response to the reviewer's comment here (as well as to reviewer #3's comments), we have whited out non-significant correlations on all correlation maps; we have also changed the value-based color scale to a significance-based color scale: color thresholds now correspond to the 10%, 5%, 1%, 0.1% levels of correlation significance, so that readers can better assess the significance of the correlations displayed.

3. I like the climate change analysis (I even like the binned analysis in Figure 10), but I am confused about one thing. It looks like expA uses the 1971-2000 values even during the 2071-2100 period. Would the use of climatological values from the 2071-2100 period be more appropriate to address at least some aspects of the T-P correlation question (e.g., the use of these correlations on the x-axis of Figure 11b)? The authors should comment.

The reviewer is correct that expA uses 1971-2000 climatological soil moisture values throughout the simulation (1950-2100), including during 2071-2100. This was the design of the experiment (see Seneviratne et al. 2013 in the manuscript's references).

Figure 10 and 11 analyze the change in summertime temperature between present (1971-2000) and future (2071-2100) as a function of changes in precipitation between present and future, and of T-P correlations in the present. So by design plots on Figure 10b and 11b have 1971-2000 T-P correlations on the x-axis. In a way, what these figures are looking at is whether physical processes and feedbacks operating at short, interannual time scales (and responsible for present-time negative T-P correlations) bear any relevance for long term coupled temperature and precipitation change - figure 10b indicates that they do.

The GLACE-CMIP5 project includes another experiment expB, where a time-varying (over a 30-year window) climatology of soil moisture is prescribed (again, see Seneviratne et al. 2013). Thus, in that experiment, soil moisture at the end of the simulations is the climatology over 2071-2100 – as the reviewer suggests using here. However, in this experiment, prescribing soil moisture in this way means the long-term response of soil moisture to climate change, as well as the feedback of this long-term soil moisture change on surface climate, are already included (for instance, a long-term local decline in soil moisture will lead to average future warming); but the short-term feedbacks are not, since soil moisture is prescribed and not interactive. Thus we feel expB was not suited to investigate the issue we meant to analysis in this section (the consistency between short-term and long-term T-P coupling).

4. Line 251-252: "inform similarly on soil moisture versus energy-limited evaporative regimes". I don't see this. How can expA inform on soil moisture limited regimes?

What we meant was that radiation-evaporation correlations, in theory, reveal patterns of soil moisture and energy-limited evaporative regime, just like soil moisture-evaporation correlations do (see results for simulation REF). We cannot look at the latter in expA (since soil moisture is prescribed) but we can look at the former. They do reveal that evaporation is energy-limited nearly everywhere in expA.

Note that this sentence has been suppressed in the reorganization of the manuscript.

#####

Reviewer #2: The paper applies notions of climate response to land-atmosphere feedbacks to a set of CMIP5 simulations designed to isolate the role of such feedbacks in climate models in both historical and future climate scenarios. Important implications are found that, by elimination, certain areas are seen to have correlations symptomatic of land-atmosphere coupling that are in fact driven by the atmosphere alone. However, regions that do have direct feedbacks in effect demonstrate a modulation of climate warming signals via the water cycle that help explain some climate change results. The case is well presented, culminating in Fig 10.

Overall I recommend only minor revisions before publication.

L207: The "terrestrial pathway" was demonstrated by Guo et al. (2006) - this should be cited, and this idea/nomenclature should be introduced in the description of Fig 1.

We have edited the description of Figure 1 in the introduction accordingly (citing Guo et al. 2006, Dirmeyer et al. 2011).

L332-334: This statement is unsatisfyingly fuzzy. It seems this could be demonstrated with a basic slope calculation (linear regression) and/or correlation of temperature against surface energy balance terms.

We rephrased this statement. What we meant is that Figure 8b reflects the different model sensitivities of surface temperature to incoming solar radiation in the context of a non-soil moisture-limited evaporative regime (since evaporation in expA is essentially energy-limited) – i.e. how surface temperature is diagnosed in a model given solar radiation and water availability.

L346: These positive correlations can be meaningless if the variability is small, as it is typically for temperature in tropics. One needs to consider the magnitude of variability as well (cf. Guo et al. 2006, Dirmeyer 2011).

In general, precipitation variability and temperature variability vary in opposite ways with latitude: while temperature variability is indeed low in the Tropics and maximum (in summer) at high latitude, precipitation variability is higher in the Tropics (where mean precipitation is maximum) and lower at mid/high latitudes – see Trenberth and Shea (2005), Wu et al. (2013) (references in the manuscript). Thus precipitation and temperature act to offset each other (in terms of the impact of variability on the calculation of correlations). This point is now highlighted in the presentation of observed T-P correlations that was added to the manuscript.

L358-360: More specifically, ...sensitive to the way clouds and convection are parameterized. Please "go there" in the discussion, as this is a point that needs to be hammered home.

This topic is now mentioned in section 4c and in the discussion section.

Fig 7: Please label the columns with the pairs of correlation signs corresponding to the four quadrants.

Labels were added. Figure 7 was moved to Supplementary material, as Figure S1.

Fig 9 and discussion L385-390: Please give some tabular data or otherwise make these more quantitative. The reader cannot tell much from the figures - it is difficult to synthesize visually.

To provide a more quantitative and interpretable view of the change in correlations in the future, Figure 9 was replaced by a histogram of areas of significant positive or negative change in T-P, SM-ET-, ET-T correlations between present and future in the different models. The original Figure 9 was retained as Supplementary Figure S2, as it helps to interpret the spatial patterns behind the histogram.

Sec 6: But what can we say about nature? It is not directly shown here whether these models reflect observed relationships in these quantities (obviously such validation would only be possible in a limited way, but any degree of confidence that could be demonstrated would be helpful, even if taken from other literature). Perhaps a strong call needs to go out here to better validate the land-atmosphere interactions in these models (spur on the observational community).

The goal of our study was primarily to highlight the intermodel differences in the multivariate physical relationships that underlie an emerging behavior such as T-P covariability. While the evaluation of relevant processes (convection, clouds,

land-atmosphere coupling, etc.) in climate models has been the subject of many studies (e.g., Dirmeyer et al. 2006), we are not aware of studies systematically evaluating global, interannual relationships similar to those analyzed in the present study. We leave the corresponding evaluation of these relationships with observations or observation-based products (for evaporation, radiation, soil moisture, etc.) for future studies. We do note, however, that climate models (at least in CMIP5) seem to overestimate summertime temperatures over land (e.g., Christensen and Boberg 2012, Mueller and Seneviratne 2014). The comprehensive causes of such biases are being investigated (e.g., Ma et al. 2014), but there are indications that models in these regions are too dry (in terms of precipitation and/or evaporation) and that subsequent soil moisture-temperature coupling contributes to the warm bias (Christensen and Boberg 2012, Mueller and Seneviratne 2014). As we mention in the text, our view is that it is thus possible that these climate models, being biased towards a dry/warm state in summer, overestimate summertime soil moisture-atmosphere interactions in general, and the role of these interactions in T-P correlations in particular.

This discussion was modified in the text – lines 568-599 in the new manuscript.

Christensen, J. H., and F. Boberg (2012), Temperature dependent climate projection deficiencies in CMIP5 models, *Geophys. Res. Lett.*, 39, L24705, doi:10.1029/2012GL053650.

Dirmeyer, Paul A., Randal D. Koster, Zhichang Guo, 2006: Do Global Models Properly Represent the Feedback between Land and Atmosphere?. *J. Hydrometeor.*, 7, 1177–1198.

Ma, H.-Y., and Coauthors, 2014: On the Correspondence between Mean Forecast Errors and Climate Errors in CMIP5 Models. *J. Climate*, 27, 1781–1798.

Sec 6: Is there any indication of connections between model fidelity and any aspects of future projections (cf. Shukla et al. 2006)?

There seems to be a link between regional model biases and sensitivities. In summer, warm models tend to project more warming in some regions (Boberg and Christensen 2012). This kind of behavior is consistent with our Figure 10b, which shows that future warming depends on present-time land-atmosphere interactions (and precipitation change). Thus a correct representation of land-atmosphere interactions is crucial for accurate future surface climate projections.

Boberg F, Christensen JH (2012) Overestimation of summer temperature projections due to model deficiencies. *Nat Clim Change* 2:433–436. doi:10.1038/nclimate1454

Dirmeyer, P. A., 2011: The terrestrial segment of soil moisture-climate coupling. *Geophys. Res. Lett.*, 38, L16702, doi: 10.1029/2011GL048268.

Guo, Z., and co-authors, 2006: GLACE: The Global Land-Atmosphere Coupling Experiment. 2. Analysis. *J. Hydrometeor.*, 7, 611-625, doi: 10.1175/JHM511.1.

Shukla, J., T. DelSole, M. Fennessy, J. Kinter, and D. Paolino, 2006: Climate model fidelity and projections of climate change, *Geophys. Res. Lett.*, 33, L07702, doi:10.1029/2005GL025579.

I do not wish to remain anonymous. -Paul Dirmeyer

#####

Reviewer #3: Review of "Interannual Coupling Between Summertime Surface Temperature and Precipitation: Processes and Implications for Climate Change" by A. Berg et al.

Summary

This manuscript includes analysis of multi-year summer-mean correlations of continental precipitation (P) and surface temperature (T) in five coupled OAGCM simulations of CMIP5 historical 20th century climate and projected 21st century climate, where the latter assumes an "RCP8.5 scenario" of greenhouse gas concentrations. For each model, the historical and projected future climate simulations are implemented in two experimental configurations, one which included interactive soil moisture ("REF") and the other with prescribed climatological soil moisture ("expA").

Major Comments

The analysis of these unique, paired simulations is quite interesting, and reflects considerable scientific insight. The description of results and their interpretation are also generally well written. However, in my opinion, the manuscript falls

short in several respects:

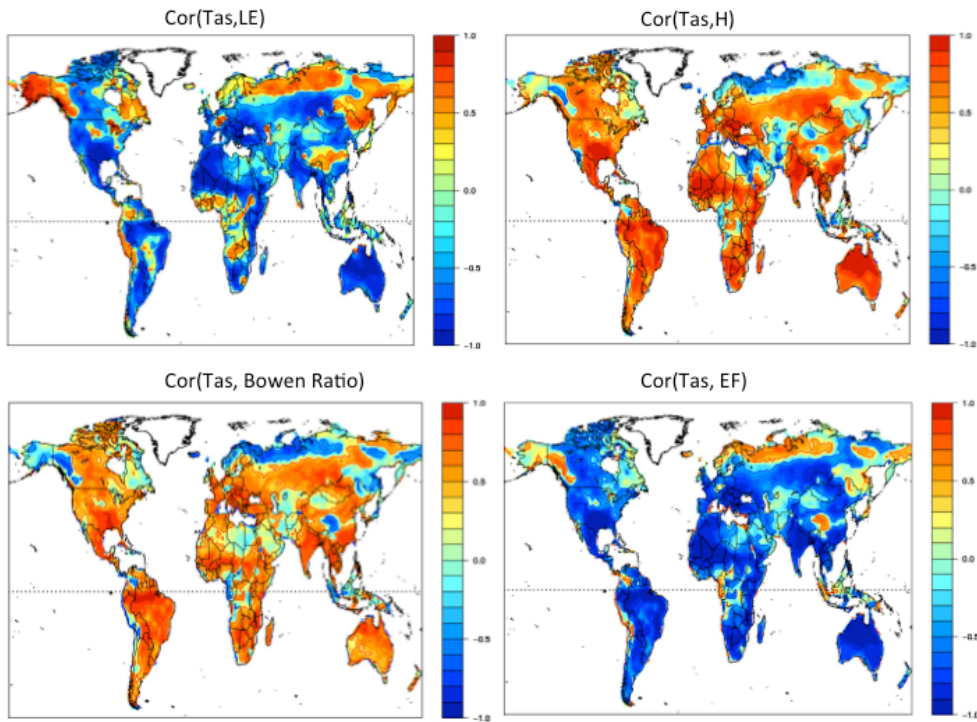
1) There is no attempt to validate the historical simulations of P-T correlations relative to those determinable from the several continental P and T observational data sets (e.g. CRU, GPCP, University of Delaware, T products from reanalyses, etc.) that are now available. This also would require the remapping of model results to a common horizontal grid that is appropriate for comparison with the available observations. A validation relative to different observational P and T data sets also would convey the degree of observational uncertainty that currently exists. Such observational validation is a necessary prerequisite to further diagnosis of model processes, since it provides guidance on how important such processes are for obtaining a "good" simulation, and on how much "weight" to give the process relationships simulated by a particular model.

Since we refer to observed T-P correlations in the introduction, in the interest of clarity (and because the observational correlations displayed in Trenberth and Shea 2005 and other papers referenced in the initial manuscript are computed slightly differently than in our study), we have added our own calculation of T-P correlations from observations in the revised manuscript (Figure 1 and lines 81-100 in the new manuscript). As recommended by the reviewer here, different observational data sets (crossing different T and P products) were used; patterns are generally robust across datasets; significance of the correlations depends on record length.

We agree that adding observations facilitates the understanding of our study by the reader and provides some context to interpret our results. However, while we understand the reviewer's request to then validate simulated T-P correlations against these observations, we believe a thorough validation (beyond general visual comparison) is beyond the scope of the study (e.g., see Wu et al. 2013), and would not necessarily add much to the analysis of the underlying physical processes in the models. Indeed, in general, a model may display the "right" observable field for the "wrong" physical reasons (and vice-versa). Another issue is the limited number of models involved here. For instance here ESM2M and EC-EARTH display the strongest negative T-P correlations (in REF), but the analysis shows that they do so through different processes. Similarly, MPI-ESM, although it shares some process-level similarities with EC-EARTH, displays lower correlations. We thus do not believe, in particular given the limited number of models here, that T-P validation would be useful here to validate processes – rather, we emphasize in the discussion the need for process-level observational constraints on models in order to resolve these uncertainties.

2) The diagnosis of differences in P-T correlations among the model simulations is limited to consideration of their relationship to only a few other simulated processes (chiefly, surface evapotranspiration ET, downward shortwave radiation SW, and soil moisture SM), leaving the authors to speculate vaguely on other unexamined processes (e.g. clouds, precipitable water, surface turbulent fluxes) that might "explain" the model differences. It is puzzling why these variables, as well as other potentially relevant processes such as surface net radiation (the main energy forcing and proportional to potential evaporation) and Bowen ratio, are left unexamined.

We would like to underscore here that we analyzed more variables and processes than shown and discussed in the manuscript (including the ones mentioned in the reviewer's comment). We could not realistically show all variables analyzed (we note that reviewer #1 already finds the study too long); all the more that some of the variables are also clearly redundant: for instance, cloud cover and incoming shortwave radiation at the surface are strongly anti-correlated (at the spatio-temporal scales analyzed here), since cloud cover essentially blocks solar radiation. We thus showed the relationship of precipitation and temperature with solar radiation (figure 8, in the original manuscript) and chose not to show corresponding relationships with cloud cover (e.g., as indicated lines 331-335 in the original manuscript). Similarly, we believe that surface turbulent fluxes are already an integral part of the study, given that i) we showed results for evapotranspiration ET, which is essentially interchangeable with the latent heat flux in this analysis, and ii) in the analysis of land evaporative regimes where ET is analyzed, the relationships between ET and soil moisture/atmosphere already carried most of the information on the 'terrestrial pathway' (Figure 1). This is because – at the time scale analyzed here – latent and sensible fluxes are significantly anti-correlated in soil –moisture limited regimes and positively correlated in energy-limited regimes. For instance below we show the correlations of temperature with, respectively, latent heat flux, sensible heat fluxes, Bowen Ratio and evaporative fraction in the GFDL model ESM2M. One can see the correlation patterns are essentially the same (with different signs). We thus feel the essential physical information is already provided by the analysis of ET in our study, without obvious need to display results for sensible heat flux or turbulent flux composites (EF, Bowen ratio).



Correlations between summer-averaged temperature (T_{as}) and latent heat flux (LE , upper left), sensible heat flux (H upper right), Bowen Ratio (lower left) and Evaporative Fraction ($EF=LE/(H+LE)$, lower right), over 1971-2000, in $ESM2M$; JJA in northern hemisphere and DJF in southern hemisphere. Contour lines indicate significant correlations (5% level, $r=0.36$).

We did also investigate net radiation in our analysis. However net radiation was not the most relevant variable for the processes analyzed here when we were interested in the role of radiation: for instance, the correlation of net radiation with ET does not reveal the patterns of soil moisture-limited and energy-limited evaporative regimes the way correlations between ET and solar radiation do (see fig.5a in the original manuscript, with negative and positive patterns – in contrast, net radiation- evaporation correlations tend to be positive everywhere). Similarly, the ‘atmospheric pathway’ for negative T-P correlations (e.g., Figure 8 in the original manuscript) involves the forcing effect of shortwave radiation on surface temperature (surface heating by radiation) and the anticorrelation between precipitation and shortwave radiation (clouds blocking radiation): other radiative fluxes cannot, a priori, play a similar role. We did investigate Figure 8 with different radiative terms (or combinations thereof, including net radiation) or directly with cloud cover: none provided a better fit (in terms of black contours and negative T-P correlations in expA on Figure 8c) than solar radiation. Note that incoming longwave radiation, for instance, tends to be positively correlated with precipitation and cloud cover, so cannot account for negative T-P correlations (since it is also positively correlated to surface temperature). Similarly, net radiation also includes the upward longwave radiation flux, function of surface temperature: thus it cannot be really considered as forcing surface temperature (which is what we were interested in our analysis here: how radiation forces surface temperature). For all these reasons we focused chiefly on solar radiation.

Finally, we do speculate in lines 353-356 about the role of precipitable water in positive T-P correlations in some models in the Tropics. Precipitable water was not a standard output in the GLACE-CMIP5 project, and therefore was not provided for the different models: investigating the related processes in the different models was thus impractical. In addition, the positive T-P correlations at equatorial latitudes were not the main focus of the present study and represent a small (and uncertain) part of the signal. In this context, we felt it was not unreasonable to limit the analysis to physical speculations. A more comprehensive study of the different positive and negative domains on Figure 6a is planned as a future study.

To account for the reviewer’s comment, we have tried to clarify in the revised manuscript why we focus on particular variables in our analysis – e.g., lines 276-281 in the new manuscript. We also added a discussion of the role of longwave radiation in (former) Figure 8 (lines 317-327 in the new manuscript).

3) The related processes that are diagnosed are depicted in ingenious (although rather complicated) ways, but it is often not easy for the reader to interpret the results. For example, in some figures it is difficult to discern differences among the

models because statistically significant correlations are not clearly differentiated. The question of what constitutes a "significant" result is also not critically examined, especially when coherent spatial patterns of significant correlations are identified in some model fields. In such cases, "field significance" (e.g. see Livesey and Chen, 1983 Mon. Wea. Rev.) is potentially a pertinent issue, at least for precipitation and other variables that are correlated with temperature, which is likely to exhibit high spatial correlation on neighboring grid cells. More careful attention to such statistical complexities is called for.

Following the reviewer's suggestion (as well as reviewer #1's suggestion), we have whited out non-significant correlations (at the 10% level) on all correlation maps; in addition, we have also changed the value-based color scale to a significance-based color scale. Color thresholds now correspond to the 10%, 5%, 1%, 0.1% levels of correlation significance (instead of regular 0.1 increments), so the reader can more easily assess the significance of the correlations that are represented.

For T-P correlations (both in observations and in models), field significance was assessed, following Liveley and Chen 1983, by using a Monte Carlo approach: the 30 yearly maps of T and P (corresponding to summer averages) were shuffled randomly 1000 times, and the area of significant T-P correlations (as percentage of the land surface) calculated each time. The field-significance threshold was then estimated as the 95% quantile of the corresponding distribution of significant areas. Note that keeping yearly maps unchanged while shuffling years retains the spatial auto-correlation within each field. This is indicated in the caption of Figure 1 in the new manuscript.

We assessed the field significance for observational and model-simulated T-P correlations, given the exploratory nature of the analysis. We did not perform the calculations for process-level correlations in models (e.g., SM-ET correlations), given that they correspond to well-established climate processes in models and corresponding correlations are generally widespread.

These general points are elaborated in more detail below.

Details

Lines 159-160: Remapping to a common grid that is compatible with available observations (taking more than one combination of observed P and T) is recommended. This is essential for model validation purposes?see Major Comments, point 1 above.

Please see reply above (point 1).

Discussion and conclusion section: See Main Comments, point 2 above. A more comprehensive analysis of other model variables that are potentially relevant to T-P correlations is needed.

Please see reply above (point 2).

Fig. 2: In this and other figures where significant correlations are the focus of attention, the 5% significance value should be stated (see remarks above on field significance, which may require a more stringent significance level?see Major Comments, point 3 above). I also would recommend "whiting out" the regions where the correlations are not significant, rather than depicting them in shades of green, while retaining a monochrome red or blue color to denote positive or negative significant correlations, respectively. This will make it much easier for the reader to focus on what is really important in the maps.

Please see reply above (point 3). We do think there is value in showing how correlations vary above the significance level: as a result, instead of retaining a monochrome red or blue color to denote positive or negative significant correlations, we use different shades of red and blue to denote different significance levels.

Fig. 3: Using a different color scheme in panels b and d would help differentiate their content from that of panels a and c. Because we now indicate areas of significant (positive or negative) T-P correlations on Figure 2, we only kept figure 3d in the revised version (Figure 3a and 3b would be redundant with these numbers).

Figs. 4 and 5: See Fig. 2 recommendations above. Adding labels to differentiate the map types of column a vs. column b also would be helpful for the reader.

Labels were added.

Fig. 6: These plots are quite difficult to interpret. To simplify, I'd recommend leaving out all non-significant points (again, the statistical significance level should be stated in the caption?see also remarks above on field significance) and using a different color scheme for the plots of column b (which are different in kind from those in column a).

We have tried to clarify the explanation for these plots in the text. For this particular plot (Figure 6a), we think it is interesting to show how T-P correlations behave in the 'phase space' (i.e., as a function of SM-ET and ET-T correlations) even below the significance level: how correlations become bluer (i.e., more negative) towards the bottom-right and upper-left corners, redder towards the bottom-left and upper-right corners (depending on models). As a result we did not white out

pixels below the 5% significance level (for T-P correlations).
The 5% significance level (for T-P correlations) was added in the captions.
Different color schemes are now used for columns a and b.

Fig. 7: Each column should be labeled--e.g. the leftmost column might be designated as "Fig. 6a Upper Left Quadrant (-, +)", with corresponding modifications of the figure caption. See also remarks above concerning field significance. A continuous blue-to-red color bar need not be used--only monochrome blue or red to differentiate positive and negative P-T correlations.

Labels were added. Please note that Figure 7 has been changed to Supplementary Figure S1.

Pixels on Figure 7 already correspond to grid cells where SM-ET and ET-T correlations are both significant (either positive or negative, depending on the quadrant). These pixels are very few for the upper-right and lower-left quadrants (with variations between models): we mention so in the text, and that therefore significance may be an issue. Beyond this statement, however, we are not aware of a practical way to quantitatively assess the field significance of a field of joint correlations.

To facilitate the interpretation of these maps and their connection to the binned plots, we have contoured areas of significant T-P correlations on this quadrant maps. We believe it is also important to show the value of T-P correlations on these grid cells for each model (and not only monochrome colors), whether these correlations are significant or not, so that readers can understand why the different models display different average T-P correlation values in the corresponding quadrants of the binned plots. Background land maps were also changed to gray (and interior borders were suppressed) to make the plots more readable.

Fig. 8: See Fig. 2 recommendations above. In panel c), the black contours are difficult to discern, but this may become easier if the non-significant values are removed from the maps (again, field significance may be an issue here).

Non-significant pixels were whited-out. Background land maps were changed to gray (and interior borders were suppressed) to make the plots more readable.

The field significance of T-P correlations in exp1A is discussed earlier in the (revised) manuscript.

Fig. 9: Future-Present correlation differences are difficult to interpret (as evidenced by a color bar that extends to absolute values > 1.0 (what are these maximum/minimum values?). It may therefore be necessary to include maps of the future correlations as well, or to find a different means to communicate the intended results. See also Fig. 2 recommendations above.

This figure showed a plot of differences in 2 correlations (each with a $[-1, 1]$ range), therefore the potential range was $[-2, 2]$: it was further narrowed to the range of actual correlation differences found in the models.

To provide a more quantitative and global view of the change in correlations in the future (as recommended by reviewer #2, too), Figure 9 was replaced by a histogram of surface area of significant positive or negative changes in T-P, SM-ET, ET-T correlations between present and future in the different models. The original Figure 9 was retained as Supplementary Figure S2, as it helps interpret the spatial patterns behind the histogram (non-significant changes were whited out).

Fig. 10: P units should be stated in the caption.

Added.

Minor Comments

Line 44, and elsewhere: Use of terms such as "interannual timescales", "interannual correlations", etc. is subject to misinterpretation. The quantities in question are zero-lag point-wise correlations of one seasonal-mean surface field against another, where these statistics are calculated over 30 years. Unless some care is taken in explaining this fact, a reader might erroneously think that "interannual correlations" are calculated with one variable field lagging the other by a whole year.

This was clarified in the text (new Figure 1 caption, Methods).

Line 139: The RCP8.5 scenario should be described in somewhat more detail.

A few words were added to remind readers that RCP8.5 is a high-energy consumption, no-climate policy and unabated-emissions scenario (akin to the SRES A2 scenario).

Line 146-147: The EC-EARTH model has been developed by a consortium, with coordinating headquarters located in Italy (see <http://www.to.isac.car.it/ecearth>). The atmospheric model component is that of the ECMWF.

Ok, changed.

Lines 221: This is the case in the Tropics? Is evapotranspiration energy-limited in the Tropics because rainfall is so plentiful, in spite of high net surface radiation?

Yes, evapotranspiration becomes energy-limited (or demand-limited) when it is no longer soil water-limited (supply-limited). Water is no longer limiting for ET in the (deep) Tropics (e.g., see Jung et al. 2010).

Jung, Martin, et al. "Recent decline in the global land evapotranspiration trend due to limited moisture supply." *Nature* 467.7318 (2010): 951-954.

Line 228: "exactly complementary"? largely or mostly complementary is a more apt description
This sentence was removed in the reorganization of the manuscript.

Lines 349-352: We speculate that? In principle, it should be possible to demonstrate this supposition using model output variables. See Main Comments, point 2 above.

Please see reply above (point 2).

Line 374: The reader should be reminded here that it is an RCP8.5 future scenario that is being simulated.

OK, added.

Line 404: Suggested rewording: "Because maps of T-P correlations show regionally limited future changes, we investigate the relationship? in the models in a binned grid-cell framework."

We reworded this part for clarity (albeit differently than suggested here).

Lines 415-417: This statement doesn't seem to apply to the IPSL model.

As indicated in the text, this statement only applies to some models (mostly ESM2M, to a lesser extent MPI-ESM and EC-EARTH).

Lines 429-430: By "the most negative T-P correlations?" do you mean both the most numerous and the largest average negative value?

Yes, both in extent and intensity (see figure 3a, c, d).

Line 436: (except maybe in MPI-ESM). What is the basis for this statement?

MPI-ESM still seems to display maximum warming in the bottom-left part of Figure 11b.

Typographical Corrections

Line 291: A paragraph break is recommended at the sentence beginning "To help interpret?"

Added.

Line 296: (far-left column)

Added.

Line 306: energy-limited almost everywhere?

Changed.

Line 311: (originating either from?)

Edited.

Line 320: add phrase "than shown here" after ?with radiation.

This part was rephrased to clarify the meaning.

Line 350: Clapeyron

Edited.

Line 363: ?do not appear to be as significant?

Edited.

Lines 431-432: ?in the present-day climate

Edited.

Line 436: ?rather than radiation impacts

Edited.

Line 459: ?which shows the most extensive and strongest negative T-P correlations?

Edited.

Line 474: ?also inherently includes (strike "in itself")

Edited.

Line 549: Mitigation (remove hyphen)

Edited.

1 **Interannual coupling between summertime surface temperature and precipitation over**
2 **land: processes and implications for climate change**

3

4 Alexis Berg^{1,2*}, Benjamin R. Lintner¹, Kirsten Findell³, Sonia I. Seneviratne⁴, Bart van den
5 Hurk⁵, Agnès Ducharne⁶, Frédérique Chéruy⁷, Stefan Hagemann⁸, David M. Lawrence⁹, Sergey
6 Malyshev¹⁰, Arndt Meier¹¹, Pierre Gentine¹²

7

8 ¹*Rutgers, The State University of New Jersey, New Brunswick, NJ, USA*

9 ²*now at International Research for Climate and Society (IRI), the Earth Institute at Columbia*
10 *University, Palisades, NY, USA*

11 ³*Geophysical Fluid Dynamics Laboratory, Princeton, NJ, USA*

12 ⁴*ETH Zürich, Zürich, Switzerland*

13 ⁵*KNMI De Bilt, The Netherlands*

14 ⁶*UMR METIS, UPMC/CNRS, Paris, France*

15 ⁷*LMD/IPSL, Université Pierre et Marie Curie, Paris, France*

16 ⁸*Max Planck Institute for Meteorology, Hamburg, Germany*

17 ⁹*NCAR, Boulder, Colorado, USA*

18 ¹⁰*Princeton University, Princeton, NJ, USA*

19 ¹¹*Centre for Environmental and Climate Research, Lund University, Lund, Sweden*

20 ¹²*Columbia University, New York, NY, USA*

21 _____

22 *Corresponding author: Alexis Berg, *International Research for Climate and Society (IRI), the*

23 *Earth Institute at Columbia University, 61 Rt 9W, Palisades, NY, USA*

24 Email: aberg@iri.columbia.edu

25 **Abstract.** Widespread negative correlations between summertime-mean temperatures and
26 precipitation over land regions are a well-known feature of terrestrial climate. This behavior has
27 generally been interpreted in the context of soil moisture-atmosphere coupling, with soil moisture
28 deficits associated with reduced rainfall leading to enhanced surface sensible heating and higher
29 surface temperature. The present study revisits the genesis of these negative temperature-
30 precipitation correlations using simulations from the Global Land-Atmosphere Coupling
31 Experiment - Coupled Model Intercomparison Project phase 5 (GLACE-CMIP5) multi-model
32 experiment. The analyses are based on simulations with 5 climate models, which were integrated
33 with prescribed (non-interactive) and with interactive soil moisture over the period 1950-2100.
34 While the results presented here generally confirm the interpretation that negative correlations
35 between seasonal temperature and precipitation arise through the direct control of soil moisture on
36 surface heat flux partitioning, the presence of widespread negative correlations when soil moisture-
37 atmosphere interactions are artificially removed in at least two out of five models suggests that
38 atmospheric processes, in addition to land surface processes, contribute to the observed negative
39 temperature-precipitation correlation. On longer timescales, the negative correlation between
40 precipitation and temperature is shown to have implications for the projection of climate change
41 impacts on near surface climate: in all models, in the regions of strongest temperature-precipitation
42 anti-correlation on interannual timescales, long-term regional warming is modulated to a large
43 extent by the regional response of precipitation to climate change, with precipitation increases
44 (decreases) being associated with minimum (maximum) warming. This correspondence appears to
45 arise largely as the result of soil-moisture atmosphere interactions.

46

47 **1) Introduction**

48 Temperature and precipitation are arguably the two most critical components of surface climate
49 over land for both terrestrial ecosystems and human society. The covariability between these two
50 variables and the processes that control or modulate it are thus of great interest to the study of the
51 terrestrial climate variability and change and associated impacts on natural and human systems.
52 One issue worth exploring is the extent to which mechanistic understanding of such relationships
53 can inform the interpretation of climate model simulations across multiple temporal and spatial
54 scales and enhance predictive skill.

55 Anti-correlation of terrestrial surface temperature and precipitation has been observed over a
56 range of time scales and regions in many prior studies. Using station data over 1897-1960, Madden
57 and Williams (1978) demonstrated that seasonal mean temperature and precipitation are negatively
58 correlated in summer over most of North America, especially over the central Great Plains, while
59 correlations of both sign were found roughly equally in other seasons. Similarly, over Europe
60 correlations were found to be positive in winter and negative in summer. Analogous results have
61 been reported using monthly data over North America for the period 1905-1984 (Zhao and Khalil
62 1993) and in regional studies over Europe (Trout 1987, Rebetz 1996) and South America
63 (Rusticucci and Penalba, 2000). More recently, Trenberth and Shea (2005) employed reanalysis
64 data and global precipitation observations to extend these results globally: while over the ocean
65 interannual correlations between summertime-monthly temperature and precipitation anomalies
66 tend to be positive, reflecting forcing of precipitation by ocean surface temperature, widespread
67 negative correlations (from the Tropics to the high latitudes) are found over land in summer in
68 both hemispheres. Adler et al. (2008) and Wu et al. (2013) have since demonstrated comparable
69 results using different global observation datasets. Although the studies mentioned above indicate
70 distinct behavior in terrestrial temperature-precipitation covariability for different seasons, Déry

71 and Wood (2005) also report significant anti-correlations between annual-mean temperature and
72 precipitation over land for observations over the 20th century. In addition, Madden and Williams
73 (1978) and Déry and Wood (2005) indicate that such relationships hold across time scales ranging
74 from monthly to decadal. It is thus possible that they modulate trends associated with climate
75 variability or global warming. For instance, Portman et al. (2009) suggest that a positive trend in
76 precipitation over recent decades may account for the postulated “warming hole” in the
77 southeastern U.S.

78 Figure 1 illustrates these temperature-precipitation correlations over land in summer in a variety
79 of observation datasets – including those used in the studies mentioned above (Trenberth and Shea
80 2005, Adler et al. 2008, Wu et al. 2013). All datasets are linearly detrended to remove effects of
81 potential trends on correlations and focus on interannual variability. Extensive significant negative
82 correlations dominate over land. The general patterns are robust across datasets: areas of strongest
83 negative correlations include the Sahel, Southern Africa, Australia, India, parts of North America,
84 South America and Eurasia. Correlations tend to be less significant for shorter records (30 years)
85 than longer records (110 years). For shorter time periods, despite general pattern agreement, there
86 are uncertainties between datasets regarding the total extent of these negative correlations (from
87 32.2% to 49.7% of land area). Where correlations are not negative, they are generally insignificant:
88 this is the case mostly in deserts, in some regions at high latitudes and in the deep Tropics. Small
89 areas of positive correlations can be found along the Equator, in particular in tropical Africa, in the
90 longer records; however, these patterns appear less robust across datasets, and while field
91 significance (e.g., Livezey and Chen 1983) is achieved for temperature-precipitation correlations
92 as a whole in all datasets, positive correlations are not field-significant if considered separately
93 (note that in that case, the threshold for field significance is slightly more than half the value
94 indicated on Figure 1). Note that while temperature variability is lower at tropical latitudes,

95 precipitation variability tends to be higher in absolute terms (the opposite being true at higher
96 latitudes; e.g., Trenberth and Shea 2005): across latitudes precipitation and temperature thus act to
97 balance each other in terms of the impact of variability on the calculation of correlations.

98 That summers over land tend to be either warm and dry or cold and wet—but typically not warm
99 and wet or cold and dry—may be interpreted *a priori* as the result of several candidate processes,
100 as depicted schematically in Figure 2. First, covariability between summertime temperature and
101 precipitation may simply emerge from synoptic scale correspondence between decreased cloud
102 cover/precipitation and increased incoming shortwave radiation heating the surface during clear-
103 sky conditions, and conversely, increased cloud cover and decreased surface heating and
104 associated temperatures during rainy conditions. Second, local land-atmosphere interactions,
105 which are expected to play a stronger role in summer (Entekhabi et al. 1992, Koster et al. 2004,
106 Seneviratne et al. 2010), may induce such relationships on seasonal scales through the effect of
107 precipitation on soil moisture and attendant surface heat fluxes. Lower rainfall, for instance, is
108 associated with reduced soil moisture and latent heat flux, and thus increased sensible heating at
109 the surface, resulting in higher near-surface air temperatures (and conversely, higher precipitation
110 is associated with lower temperature). Note that this pathway corresponds to the ‘terrestrial
111 branch’ of soil moisture-atmosphere interactions (Guo et al. 2006, Dirmeyer et al. 2011). Positive
112 feedbacks of modified surface heat flux partitioning on cloud cover/ radiation (e.g., Gentine et al.
113 2013) and large-scale circulation (e.g., Haarsma et al. 2009) may further amplify the effect of
114 precipitation variability on temperatures.

115 The impact of soil moisture anomalies on subsequent temperatures has been highlighted in a
116 number of mechanistic modelling studies that have isolated soil moisture variability as a source of
117 daily surface temperature variability in summer, especially in transitions between humid and dry
118 climates (Koster et al. 2006, Seneviratne et al. 2006, Koster et al. 2010). Observation-based

119 estimates of soil moisture-temperature coupling are consistent with these patterns (Miralles et al.
120 2012). Soil moisture-atmosphere interactions have been shown to play an amplifying role in warm
121 extremes, as noted for recent European heat waves in observational (Vautard et al. 2007, Hirschi et
122 al. 2011, Quesada et al. 2012) as well as modelling (Fischer et al. 2007, Zampieri et al. 2009)
123 studies. Observations provide support for antecedent soil moisture deficits enhancing the
124 probability of subsequent summer hot conditions across different regions of the globe (Durre et al.
125 2000, Shinoda and Yamaguchi 2003, Mueller and Seneviratne 2012).

126 These lines of evidence point to coupled land-atmosphere processes as the source for the
127 regionally widespread anti-correlations of summertime terrestrial temperature and precipitation
128 (Trenberth and Shea 2005, Koster et al. 2009). However, whether local land-surface processes are
129 solely responsible for the large-scale, interannual covariability between summertime-averaged
130 temperature and precipitation as depicted in Figure 1 (see also Trenberth and Shea 2005, Adler et
131 al. 2008 and Wu et al. 2013), remains to be determined. In their analysis of the relationship
132 between mean summertime temperature and precipitation using a single climate model, Koster et
133 al. (2009) indicate that these temperature-precipitation anti-correlations “essentially disappear”
134 when simulated land-atmosphere interactions are disabled by prescribing surface fluxes; they thus
135 identify land-atmosphere processes as the dominant driver of these relationships. Krakauer et al.
136 (2009) also report reduced coupling of temperature and precipitation in another model when soil
137 moisture-atmosphere coupling is suppressed through prescribing soil moisture, although they did
138 not investigate this behavior in detail.

139 The aim of the present study is to explore more extensively, across several models, the
140 correlations between mean temperature and precipitation in order to untangle the contribution of
141 the different processes illustrated in Figure 2. To do so, we make use of simulations from the
142 recent CMIP5 Global Land-Atmosphere Coupling Experiment (GLACE-CMIP5; Seneviratne et al.

143 2013), in which simulations spanning 1950-2100 were performed with a suite of current-
144 generation models following an experimental set-up disabling land-atmosphere interactions. The
145 manuscript is organized as follows: we describe the models and fields analyzed in Section 2.
146 Section 3 presents the temperature-precipitation correlations in the GLACE-CMIP5 simulations.
147 Land and atmospheric controls on these correlations are investigated in section 4, while section 5
148 describes the potential relevance of these correlations for climate change projections. The principal
149 results and implications of our study are discussed in Section 6.

150

151 **2) Methods and datasets**

152 In the context of the GLACE-CMIP5 experiment, five modeling centers performed a land-
153 atmosphere-only transient climate change simulation (hereafter referred to as “expA”) in which
154 total soil moisture was overridden in the respective models by the climatological values over 1971-
155 2000 from the corresponding historical, fully coupled CMIP5 simulation. ExpA extends over
156 1950-2100, with transient sea surface temperatures (SSTs), sea ice, land use, and radiative forcing
157 agent concentrations prescribed from the corresponding CMIP5 simulations (using the historical
158 simulations over 1950-2005 and the RCP8.5 scenario thereafter, characterized by high population
159 and energy consumption growth, no climate policy and unabated emissions); however, soil
160 moisture in each model is overridden by the 1971-2000 climatological seasonal cycle of soil
161 moisture, and thus maintains a climatological seasonal cycle throughout the transient simulation.
162 For each model, either the fully coupled CMIP5 simulation, or, in cases where there were minor
163 differences in set-up, a new reference simulation identical to expA but with interactive soil
164 moisture, was considered as a reference simulation (hereafter referred to as “REF”). The five
165 models analyzed here are Geophysical Fluid Dynamic Laboratory’s ESM2M, National Center for
166 Atmospheric Research’s CCSM4, the EC-EARTH model developed by a consortium of European

167 research institutions¹, MPI-ESM from Max Planck Institute for Meteorology, and Institut Pierre
168 Simon Laplace's IPSL-CM5A. The reader is referred to Seneviratne et al. (2013) for further
169 discussion of the models and the experimental protocol of GLACE-CMIP5.

170 Here we compare interactive (REF) and prescribed (expA) soil moisture simulations over 1971-
171 2000; we focus on correlations between temperature (T) and precipitation (P) in summer
172 calculated, as in Figure 1, as zero-lag point-wise correlations of summertime-mean temperature
173 against precipitation (hereafter referred to as T-P correlations). Although focusing on 1971-2000
174 limits sample sizes to 30 paired values (temperature and precipitation for 30 summers), it ensures
175 that both simulations have identical soil moisture climatologies. The comparison thus isolates the
176 effect on climate of soil moisture variability and associated soil moisture-atmosphere interactions
177 only. June-July-August (JJA) means are used for the Northern Hemisphere and December-
178 January-February (DJF) means for the Southern Hemisphere. Correlations between other variables
179 are investigated similarly. As in Figure 1, 30-year time series of all climate variables analyzed
180 were linearly detrended to remove any spurious effect of climate change-related trends on
181 correlations and focus on interannual variability; such detrending was found to have little
182 quantitative impact on the results for most models. Correlations are presented on the models'
183 native grids, with resolution ranging from 1.125° x 1.125° for EC-EARTH to 3.75° x 1.875° for
184 IPSL-CM5A. Antarctica and Greenland are removed from all datasets.

185

186 **3) Temperature-Precipitation correlations**

187 Figure 3a shows that T-P correlations are generally significantly negative over most of the land
188 surface in REF in all models. The common patterns of negative T-P correlations that emerge
189 across models - e.g., the US, the Sahel, a large swath of Eurasia and parts of Southeast Asia in JJA;

¹ See www.to.isac.cnr.it/ecearth/

190 the Amazon, South Africa and Northern Australia in DJF- are in qualitative agreement with
191 calculations based on observations (Figure 1). Trenberth and Shea (2005) and Wu et al. (2013)
192 indicate similar general agreement from other coupled climate models. Beyond common patterns,
193 Figure 3a shows that the strength and extent of these correlations vary across models, from strong
194 and widespread correlations (EC-EARTH) to weaker and more diffuse correlations (CCSM4).
195 When combining correlation extent and strength, EC-EARTH shows the strongest negative
196 correlations, followed by ESM2M, MPI-ESM, IPSL-CM5A and CCSM4 (Figure 4).

197 As in observations, areas of positive correlations in models are much reduced compared to areas
198 of negative correlations. However, two models (ESM2M, CCSM4) exhibit coherent patches of
199 significant positive correlations along the Equator, over Central Africa and Indonesia, which are
200 reminiscent of areas of positive correlations found in some observational datasets (Figure 1). In
201 ESM2M at least, positive correlations achieve field significance (4.2% of land surface area, above
202 the 3.9% threshold). Thus, model uncertainty seems to parallel observation uncertainty regarding
203 the covariability of temperature and precipitation over land in equatorial regions. Overall, both
204 negative and positive correlations tend to be more significant in models (respectively, 55.4% and
205 2.4% of the land surface area on average across models) than in observations (respectively 42.8%
206 and 0.5% on average across datasets) over comparable 30-year time periods. This difference may
207 stem from observation uncertainty and the resulting difficulty in diagnosing process-level
208 relationships in observation datasets; we note that results from longer observational record are
209 more consistent with model results (respectively, 57.9% and 1.9% of land surface area
210 significantly negatively or positively correlated; see Figure 1).

211 The results for simulation expA in Figure 3b indicate that when soil moisture is prescribed,
212 negative T-P correlations are reduced, in all models, both in extent and intensity. However, while
213 in some models these correlations essentially disappear, becoming less extensive and more

214 disorganized (ESM2M, IPSL-CM5A and, to a lesser extent, CCSM4), in others extensive, spatially
215 coherent and significant negative correlations persist (MPI-ESM, EC-EARTH), often in similar
216 regions as in REF. Figure 4 indicates that in terms of combined extent and strength, negative T-P
217 correlations in simulation expA reach 52.2% and 49.2%, respectively, of those in REF in MPI-
218 ESM and EC-EARTH, but only 18.3%, 32.3% and 26.3% in ESM2M, CCSM4 and IPSL-CM5A,
219 respectively. Using this index, correlations are stronger in EC-EARTH in expA than in CCSM4 in
220 REF.

221 Positive correlations along the Equator in ESM2M and CCSM4 remain in expA, which indicates
222 that they are unrelated to soil moisture variability. We further point out that the spatial extent of
223 positive correlations increases from REF to expA (Figure 3); positive correlations achieve field
224 significance in expA in three models (ESM2M, CCSM4 and IPSL-CM5A). Small patches of
225 positive correlations appear in the Tropics in expA where insignificant or even negative
226 correlations occurred in REF: this is the case over the eastern part of South America, southern
227 Africa or Australia, in particular in IPSL-CM5A, CCSM4 and ESM2M. We note that overall,
228 despite the reduction in negative correlations from REF to expA, T-P correlations remain field-
229 significant in expA in all models.

230 Our general *a priori* interpretation of the differences between simulations REF and expA in
231 Figure 3 is that soil moisture-atmosphere interactions have been disabled in expA by the
232 suppression of interactive soil moisture. Thus, while all processes represented on Figure 2 are
233 active in REF and can contribute to simulated T-P covariability, only atmospheric processes play a
234 role in these correlations in expA, and the differences between both simulations reflect the
235 contribution of soil moisture-atmosphere interactions. To confirm this interpretation and further
236 investigate the processes underlying negative T-P correlations in both simulations, we analyze in

237 the following section the different relationships highlighted in Figure 2 in the different models, on
238 the same interannual seasonal-mean timescales as for T-P correlations in Figures 1 and 3.

239

240 **4) Land and atmospheric control on Temperature-Precipitation correlations**

241 **a. Evaporative regimes**

242 To highlight the process-level differences between both simulations, we first investigate the
243 different evaporative regimes in REF and expA. In general, evapotranspiration may be either
244 limited by soil moisture availability or by atmospheric demand (temperature, net radiation, vapor
245 pressure deficit, wind speed); soil moisture's feedbacks to the atmosphere are associated with the
246 soil moisture-limited evaporative regime, when soil moisture controls surface turbulent fluxes and
247 subsequent impacts on the low-level atmosphere (e.g., Seneviratne et al. 2010).

248 Correlations between seasonal mean soil moisture (SM) and evapotranspiration (ET) in Figure 5a
249 highlight the average summertime evaporative regime in the different models in REF. Positive
250 correlations indicate that, on average, ET is soil moisture-limited (higher soil moisture leading to
251 larger ET). This is the case, generally, in the sub-Tropics and mid-latitudes. Conversely, negative
252 correlations point out regions where ET is energy-limited: when water supply is sufficient, ET
253 variability is then determined by variations in atmospheric demand, so that ET variability then
254 drives soil moisture variability (e.g., higher ET depleting soil moisture, producing negative SM-ET
255 correlations). This is the case in the Tropics, and in high latitude and high altitude regions. Large-
256 scale patterns of SM-ET correlations are fairly consistent across models, but correlations vary in
257 amplitude and regional differences can be important. MPI-ESM noticeably exhibits the most
258 positive correlations, and shows almost no negative correlations in the Tropics. These intermodel
259 differences arguably reflect the different parameterizations of soil hydrology in the models (Koster
260 et al. 2009b).

261 Across models, patterns of correlations between summertime mean ET and atmospheric demand,
262 represented here by temperature (Figure 5b) and incoming solar (shortwave) radiation (Rs, Figure
263 5c) are consistent with the above. ET-T correlations are negative where soil moisture limits ET
264 (see Figure 5a): reduced ET is then offset by higher sensible heat flux, thus leading to higher
265 temperatures (and vice-versa, higher ET damps temperature). In these regions, negative ET-Rs
266 correlations (Figure 5c) reflect the fact that higher evapotranspiration results from higher rainfall,
267 which is associated with lower solar radiation. Conversely, ET-T and Rs-ET correlations are
268 positive where atmospheric evaporative demand, linked to temperature and surface net radiation,
269 drives evapotranspiration. Comparison between Figure 5b and 5c shows that in most models, the
270 effect of radiation seem to prevail at low latitudes and the effect of temperature at high latitudes.
271 Overall, evaporative regimes in REF as diagnosed in Figure 5 are consistent with similar analyses
272 using climate models (Seneviratne et al. 2006), observation-driven land surface models (Teuling et
273 al. 2009) or observation-based datasets (Jung et al. 2010). Note that the analysis of the surface or
274 atmospheric control on ET (i.e., latent heat flux) here illustrates the control on surface turbulent
275 heat fluxes, since at the time scale considered here the surface sensible heat flux is strongly anti-
276 correlated with ET in soil moisture–limited regimes and positively correlated in energy-limited
277 regimes. Thus results for Figure 5 are similar with either surface heat flux, or composite thereof
278 (e.g., Bowen Ratio, evaporative fraction).

279 Results from simulation REF show complementary patterns of soil moisture- and energy limited
280 evaporative regimes; by contrast, results for simulation expA (Figure 6) show that when soil
281 moisture variability is prescribed, only atmospheric control on surface ET remains. Figure 6
282 indicates that atmospheric demand (represented here by incoming shortwave radiation – results
283 with temperature are similar) are driving ET variability nearly everywhere in the different models,
284 except in desert and arid areas where there is little soil moisture to evaporate (note that since the

285 seasonal cycle soil moisture is prescribed in expA and that soil moisture is thus constant from one
286 summer to the next, correlations between soil moisture and ET, similar to Figure 5a, cannot be
287 computed for expA). This atmospheric control reflects the absence of soil moisture depletion
288 following evapotranspiration in expA, since soil moisture is overridden by climatological values at
289 every time step in the models: in this context, soil moisture exerts no control on ET, and the
290 atmosphere is left to drive ET variability.

291 The differences in evaporative regimes between REF and expA on Figures 5 and 6 confirm that
292 while the land surface can feed back to the atmosphere in REF (in regions of soil moisture-limited
293 regime), the atmosphere is entirely driving the land surface in expA. This confirms that soil
294 moisture-atmosphere interactions are playing no role in T-P correlations in simulation expA in
295 Figure 3 (in particular, in MPI-ESM and EC-EARTH). In the context of Figure 2, we thus interpret
296 negative T-P correlations in expA as resulting from the “atmospheric” pathway.

297

298 **b. Atmospheric control on T-P correlations in expA**

299 The atmospheric pathway involves covariation of cloud cover and rainfall, with reduced rainfall
300 and associated clouds (originated from either changes in large-scale circulation or in convection)
301 leading to increased surface solar radiation and increased temperature, and conversely, increased
302 precipitation/cloud cover leading to reduced incoming solar radiation and temperature. Figure 7
303 supports this interpretation by showing that regions of negative T-P correlations in simulation
304 expA in Figure 3b are generally collocated (Figure 7c) with regions where precipitation anomalies
305 are significantly anti-correlated with solar radiation anomalies (Figure 7a) and where,
306 simultaneously, radiation anomalies are significantly (positively) correlated with surface
307 temperature anomalies (Figure 7b). Admittedly, this collocation is not proof of causation: we
308 cannot rule out that a separate, different mechanism may independently generate such negative T-P

309 correlations in the models (in which case temperature-radiation and precipitation-radiation
310 correlations of opposite sign may also independently be observed, as here). However, the good
311 spatial match on Figure 7c (in particular for MPI-ESM and EC-EARTH) and the physical
312 plausibility of the underlying processes are suggestive of a direct radiative control on the T-P
313 correlation in expA. Note that radiative terms other than solar radiation play no similar direct role
314 in negative T-P correlations. In particular, downwelling longwave radiation tends to be positively
315 correlated with cloud cover and precipitation, so it would induce positive, instead of negative, T-P
316 correlations (since it heats the surface as well). This effect may actually act to oppose the impact of
317 cloud cover and solar radiation on T-P correlations: in particular, the lower negative T-P
318 correlations actually simulated by CCSM4 over large parts of Eurasia compared to the patterns of
319 precipitation-radiation-temperature covariations (black contours on Figure 7c) correspond to
320 regions where surface temperature appears more strongly associated with downwelling longwave
321 radiation in CCSM4 than in other models (not shown). Thus, our interpretation is that in this model
322 and this region, positive anomalies of cloud cover/precipitation are not clearly correlated with
323 negative temperature anomalies, because of the effect of the associated longwave radiation on
324 surface temperature.

325 As shown in Figure 3b, negative T-P correlations in expA are wider and more coherent in MPI-
326 ESM and EC-EARTH than in the other models. We interpret the differences between models as
327 reflecting the differences between models in terms of cloud/radiative processes and impacts on the
328 surface energy budget. Figure 7a shows that in simulation expA anomalies of precipitation across
329 models are consistently and extensively associated with anomalies of incoming shortwave
330 radiation of opposite signs. Differences between models mostly reflect different relationships
331 between cloud cover and precipitation, and, to a lesser extent, differences in the strength of the link
332 between cloud cover and radiation (not shown). On the other hand, positive correlations between

333 incoming shortwave radiation and temperature are less extensive; they also show more differences
334 between models (Figure 7b). These differences reflect the different sensitivities of surface
335 temperature to incoming solar radiation in the models, in particular in a non-soil moisture-limited
336 evaporative regime such as in expA (see previous subsection). For EC-EARTH, MPI-ESM and (to
337 a lesser extent) CCSM4, these differences result in large swaths of positive correlations between
338 summertime-mean shortwave radiation and surface temperature in the Tropics and high latitudes,
339 whereas similar correlations are less extensive in ESM2M and IPSL-CM5A. As mentioned above,
340 models also exhibit different relationships of surface temperature with downwelling longwave
341 radiation (in particular CCSM4). The combination of these differences in longwave/shortwave
342 radiation-temperature relationships with more minor differences in precipitation-radiation
343 correlations explains the spread in T-P correlations between models in expA (Figure 3b). Overall,
344 Figures 7a and 7b arguably reflect the aggregated effects of combined differences in parameterized
345 cloud, convection, radiation, soil and turbulence schemes between models.

346

347 **c. Land and atmospheric control on T-P correlations in REF**

348 We now focus on the processes underlying T-P correlations in the context of interactive soil
349 moisture, in simulation REF.

350 Soil moisture-atmosphere interactions arguably contribute to negative interannual T-P
351 correlations in REF where correlation patterns in Figure 3a overlap with regions of positive SM-
352 ET correlation (soil moisture controlling ET) and negative ET-T correlation (ET controlling
353 temperature) in Figure 5. To analyze this relationship, we combine information from Figures 3 and
354 5 by binning T-P correlations along SM-ET correlations and ET-T correlations. Double histograms
355 (or binned plots) on Figure 8a thus show T-P correlations in the different models in REF as a
356 function of SM-ET and ET-T correlations (over land). For each model, for a given bin of SM-ET

357 and ET-T correlation values, Figure 8a displays the average T-P correlation over all (map) pixels
358 from Figure 5a and 5b that fall within this particular bin of SM-ET and ET-T correlations; Figure
359 8b indicates the number of map pixels from Figure 5 that fall in this bin. To help interpret Figure
360 8a in a spatial sense, Supplementary Figure S1 also displays the maps of pixels belonging to the
361 different domains of the binned plots (i.e., upper-left, upper-right, lower-right and lower-left parts
362 of the plots), showing the corresponding T-P correlations.

363 All models display negative T-P correlations in the bottom-right part of the plots, which
364 corresponds to the soil moisture-limited evaporative regime: this quadrant corresponds to regions
365 where, as mentioned above, soil moisture controls evapotranspiration (positive SM-ET
366 correlations) and evapotranspiration controls temperature (negative ET-T correlations; see Figure
367 5). T-P correlations are overwhelmingly negative in these regions (see also Figure S1, far-right
368 column). This indicates that in all models, soil moisture atmosphere interactions do contribute to
369 negative T-P correlations (in REF).

370 A benefit of the binned analysis is that it shows that some models also produce negative T-P
371 correlations in the upper-left part of the plots (EC-EARTH, MPI-ESM, CCSM4 to a lesser extent).
372 This domain corresponds to the energy-limited evaporative regime: in this quadrant, temperature
373 drives evapotranspiration (positive ET-T correlations) and evapotranspiration drives soil moisture
374 (negative SM-ET correlation; see Figure 5). Figure S1 shows that, as mentioned in section 4a,
375 these regions can be found at high latitudes and in the Tropics (far-left column). MPI-ESM
376 displays negative T-P correlations predominantly at high latitudes, while EC-EARTH does so
377 mostly in the Tropics (CCSM4 as well, but over the Amazon only). Since evapotranspiration in
378 this regime is driven by atmospheric demand and drives soil moisture variability, negative T-P
379 correlations in this quadrant clearly do not result from precipitation's impact on soil moisture and
380 soil moisture's subsequent control on evapotranspiration and temperature. Rather, we interpret

381 them as resulting from the same atmospheric processes as highlighted in the previous section in
382 simulation expA. This interpretation is supported by the consistency between Figure 8a and Figure
383 3b: the models that show negative T-P correlations in the energy-limited evaporative regime in
384 REF (upper-left part of the binned plots in Figure 8a) are the same ones that display significant
385 negative T-P correlations in simulation expA in Figure 3b (EC-EARTH, MPI-ESM, and to a lesser
386 extent, CCSM4). In both cases, the surface evaporative regime is controlled by the atmosphere (see
387 section 4a). Figures 3b and 8a thus provide two independent yet consistent lines of evidence that
388 these models are capable of producing negative T-P correlations that are not the product of soil
389 moisture-atmosphere interactions, but which emerge through atmospheric processes only.

390 Figure 8b indicates that for most models, most (map) pixels (from Figure 3a) lie in the bottom-
391 right part of the binned plots: that is, there are more map pixels that fall into the soil moisture-
392 limited evaporative regime; pixels in the energy-limited regime are comparatively less numerous
393 (except for IPSL-CM5A; see also Figure 5). More generally, Figure 8b shows that most pixels fall
394 along a general bottom-right/upper-left line. This is to be expected, as the two axes are not
395 independent: a positive SM-ET correlation for instance, reflecting a soil moisture-limited
396 evaporative regime, will tend to be associated with a negative ET-T correlation (as more
397 evapotranspiration will then cool the surface). However, Figure 8a also shows hints of coherent
398 positive T-P correlation patterns emerging across models as one departs from this central line and
399 moves towards the upper-right and lower-left quadrants, where SM-ET and ET-T correlations
400 follow different behaviors. These tend to correspond to pixels in, respectively, equatorial latitudes
401 and high latitudes (Suppl. Fig. S1). We note that these portions of the binned plots typically
402 involve a small number of pixels (Figure 8b), which are often dispersed, so limited sample size
403 may be an issue. On the other hand, as indicated in section 3, coherent patches of positive T-P
404 correlations over equatorial latitudes exist in particular in Equatorial Africa and the Maritime

405 Continent in ESM2M and CCSM4; they correspond to the bottom-left quadrant in Figure 8 (see
406 also Suppl. Fig. S1). The presence of positive correlations in both the interactive and prescribed
407 soil moisture configurations (Figure 3) indicates that these are decoupled from interactive soil
408 moisture processes. Rather, we speculate that such correlations reflect simulated Clausius-
409 Clapeyron temperature scaling of precipitable water, which in turn is tightly associated with local
410 precipitation, similar to corresponding relationships over ocean surfaces (Neelin et al. 2009, Muller
411 et al. 2009, 2011). As discussed in the introduction, there is some ambiguity in the significance of
412 the observed correlations over equatorial latitudes (Figure 1). In this context it is difficult to assess
413 the validity or realism of the simulated regional covariability in the tropics. We note that the
414 simulated tropical correlations are clearly model-dependent, likely reflecting differences in
415 parameterizations of clouds and convective precipitation between models in these regions.

416 Small coherent areas of positive T-P correlations over high latitudes corresponding to the upper-
417 right quadrant exist in particular in the IPSL-CM5A and CCSM4 models (Suppl. Fig. S1) –
418 however these positive correlations do not appear to be as significant or extensive as those in the
419 Tropics (see also Figure 3a). The upper-right quadrant corresponds to mean hydroclimatic
420 conditions under which summertime mean evapotranspiration appears to be, on average, controlled
421 by both soil moisture (positive SM-ET correlation) and temperature (positive ET-T correlation).
422 One possible explanation for this model behavior is that precipitation over these areas is associated
423 with advection of warmer, moister air: in this case, precipitation directly increases
424 evapotranspiration (because of the positive SM-ET correlation), so the latter also appears
425 associated with higher temperature.

426

427

428 **5) Implications for climate change**

429 In the previous section, we investigated the processes through which T-P correlations at the
430 interannual time scale (i.e., from one summer to the next) arise in the different climate models.
431 Taking advantage of the fact that both simulations REF and expA were simulated through 2100
432 using the RCP8.5 scenario after 2005, we now focus on how T-P correlations evolve in a warmer
433 climate and what role they play in climate change projections.

434

435 **a. Projected future T-P correlations**

436 Figure 9 shows that in all models, parts of the land surface show significantly more negative T-P
437 correlations at the end of the 21st century (2071-2100) compared to the end of the 20th century
438 (1971-2000), while correlations also become significantly more positive in other areas (note that
439 areas becoming more positive may still correspond to negative correlations). In MPI-ESM,
440 CCSM4 and IPSL-CM5A, areas where correlations become significantly more negative clearly
441 outweigh areas where significant positive changes occur, which reflects an increase in the total
442 area of significant negative T-P correlations. Similar changes are less evident for ESM2M and EC-
443 EARTH. Despite these changes, the overall spatial pattern of T-P correlations (Figure 3a) remains
444 similar in the future in the different models (not shown). We note here that we cannot assess the
445 field significance of these changes in T-P correlations between present and future through the same
446 Monte-Carlo approach as used in Figure 1 and 3, as it would require sampling a control simulation
447 with no changes in climate forcing agents. We point out that the net change (i.e., the area
448 difference between areas becoming significantly more negative and areas becoming significantly
449 more positive) remains smaller than 6% of the land surface in all models.

450 Because in all models, negative T-P correlations arise either partly or mostly as a result of soil
451 moisture's feedbacks on surface temperature (see previous section), we analyze concurrent
452 changes in SM-E and ET-T correlations. Figure 9 shows that in MPI-ESM, CCSM4 and IPSL-

453 CM5A, significant changes in SM-ET and ET-T correlations are, respectively, predominantly
454 positive and negative, which reflect an increased control of soil moisture on evapotranspiration and
455 increased control of evapotranspiration on temperature. Supplementary Figure S2 illustrates these
456 changes spatially and shows that concurrent changes in SM-ET and ET-T mainly occur at high
457 northern latitudes. This shift towards soil moisture-controlled conditions in summer in the future in
458 regions like Eastern/Northern Europe and Siberia is consistent with previous modeling results
459 (Seneviratne et al. 2006, Dirmeyer et al. 2012, Dirmeyer et al. 2013). This strengthening of the
460 land-atmosphere pathway (Figure 2) is consistent with the more negative T-P correlations in these
461 models; one must note, however, that areas of more negative T-P correlations do not necessarily
462 overlap with areas of increased soil moisture control (e.g., Central Asia in MPI-ESM). In ESM2M,
463 no such strengthening of the land-atmosphere pathway can be seen; rather, it seems that soil
464 moisture's control on evapotranspiration becomes less pronounced in the future (Figure 9 and
465 Suppl. Fig. S2). In EC-EARTH, a small shift towards more soil moisture controlled conditions is
466 projected over Eastern Europe, which appears to result in stronger negative T-P correlations over
467 this region.

468

469 **b. Regional temperature change**

470 We now investigate whether T-P covariability at the interannual time scale, such as diagnosed by
471 T-P correlations, affects long-term temperature change over land in the models. Because patterns
472 of T-P correlations show overall modest change in the future in the models (or become even more
473 negative, see previous sub-section), we use present-climate T-P correlations to investigate how
474 projected future warming is affected by interannual T-P covariability in the models. We do so
475 using a binned grid-cell framework similar to Figure 8.

476 First, Figure 10a shows the mean summertime warming projected between 1971-2000 and 2071-
477 2100 in the different models in simulation REF. Differences in the average temperature change
478 reflect differences in climate sensitivities: IPSL-CM5A shows the largest overall warming, while
479 ESM2M shows the smallest (with even some cooling in the Southern Ocean and the North
480 Atlantic). In all models, summertime warming is greater over land than over the oceans, consistent
481 with a land-sea warming ratio greater than unity (e.g., Sutton et al. 2007); however, patterns of
482 changes over land differ between models. Figure 10b helps shed light on these differences by
483 showing that the land regions of maximum warming in the models tend to correspond to regions
484 that exhibit both the highest T-P summertime anti-correlations in current climate and negative
485 projected precipitation changes. This pattern is particularly clear in ESM2M, MPI-ESM and EC-
486 EARTH, somewhat less pronounced in CCSM4 and IPSL-CM5A. A few pixels of maximum
487 warming also appear in regions of positive T-P correlations in Figure 10b (in general with positive
488 precipitation change) corresponding to large warming in desert areas (see Figure 3a). In some
489 models (ESM2M, MPI-ESM), conversely, minimum long-term warming is projected in regions
490 that exhibit both the highest T-P summertime anti-correlations in current climate and positive
491 projected precipitation changes.

492 This indicates that, consistently across models, T-P correlations have the potential to modulate
493 long-term warming in conjunction with precipitation change. This is consistent with prior studies
494 (Madden and Williams 1978, Déry and Wood 2005) showing that the T-P relationship holds over a
495 range of time scales, including decadal variability and secular trends.

496 Figure 11a shows that in the absence of soil moisture change, long-term warming is largely
497 reduced over land in expA compared to REF. This is consistent with the role of average soil
498 moisture change (between present and future) in amplifying summertime warming over land, as
499 shown in Seneviratne et al. (2013). This difference highlights the role of land-atmosphere

500 interactions in the land-sea warming contrast projected by climate models (Sutton et al 2007).
501 Figure 11b shows that in contrast to REF, no relationship similar to that in Figure 10b emerges
502 between long-term warming, precipitation change and T-P correlations in simulation expA – to the
503 exception of MPI-ESM. Interestingly, while EC-EARTH and MPI-ESM both display the most
504 negative T-P correlations in expA over 1971-2000 (both in extent and intensity, Figure 4), they
505 show different behaviors in terms of long-term warming (in expA): EC-EARTH does not exhibit a
506 relationship between future warming and T-P correlations in this simulation, while MPI-ESM
507 does. It thus appears unclear whether processes associated with the atmospheric pathway (Figure
508 2), which result in negative T-P correlations at the interannual time-scale, can also affect future
509 surface warming through concurrent long-term changes in precipitation. At the very least,
510 comparison between Figure 10b and 11b suggests that land-atmosphere interactions contribute to
511 the warming patterns in Figure 10b to a large extent. In other words, our results indicate that
512 through soil moisture feedbacks on near-surface climate, regional trends in precipitation may
513 strongly modulate regional temperature change from global warming.

514

515 **6) Discussion**

516 By comparing an ensemble of simulations with and without interactive soil moisture, we
517 investigated the mechanisms responsible for negative T-P correlations for the first time in a suite
518 of climate models. We have demonstrated that negative correlations between summertime-mean
519 temperature and precipitation can arise through two mechanistic pathways in climate models, as
520 described in Figure 2. The across-the-board decrease in T-P correlations between REF and expA in
521 Figures 3a and 3b indicate that the terrestrial pathway, i.e. the control of soil moisture on surface
522 heat fluxes and temperature, largely contributes to these correlations in all models. However, while
523 soil moisture-atmosphere interactions are the main driver in some models, in others (mainly, MPI-

524 ESM, EC-EARTH) these correlations also emerge in the absence of soil moisture-atmosphere
525 coupling (expA). Our analysis indicates that this comes in response to the stronger association in
526 these models between cloud cover and precipitation on the one hand, and between solar radiation
527 and surface temperature on the other hand. Consistently, Figure 8 shows that in the context of
528 interactive soil moisture (REF), these models are capable of producing negative T-P correlations,
529 not only in soil moisture-limited regions, but also in regions of energy-limited evaporative regime,
530 where soil moisture variability does not feed back on surface temperature. This suggests that, in
531 these models, the atmospheric pathway may also contribute to negative T-P correlations even in
532 soil moisture-limited regions: in such regions, surface temperature may also be partly driven by the
533 radiation anomalies associated with precipitation and soil moisture variability. This hypothesis is
534 supported by the fact that in MPI-ESM and EC-EARTH, areas with atmosphere-driven negative T-
535 P correlations in expA (Figure 3b) are found in the same regions that display land-driven
536 correlations in REF (this is also the case in the other models over regions such as Australia or
537 India). This suggests that atmospheric processes associating T and P (isolated in simulation expA)
538 also contribute to the negative correlations in these regions in REF in Figure 2a. This is also
539 consistent with the result that EC-EARTH, which shows the most extensive and strongest
540 correlations in REF, also displays the strongest negative correlations in expA. In other words, in
541 these models the two pathways appear to act in combination to produce strong negative T-P
542 correlations over these regions. This additivity suggests that the contribution of soil moisture-
543 atmosphere interactions to negative T-P correlations can be inferred from the difference between
544 simulations REF and expA in Figure 4. Interestingly, some regions show positive T-P correlations
545 in the absence of soil moisture-atmosphere interactions and negative T-P correlations otherwise
546 (Figure 3). This suggests that in some cases these interactions can act to oppose the atmospheric
547 regime: these regions appear to be mostly located on the eastern side of continents (in the Southern

548 Hemisphere), under the influence of air masses from the ocean; while this would result in positive
549 T-P correlations if only the atmosphere was driving T-P covariability (as suggested by Figure 3b),
550 the water-limited evaporative regime in these regions (Figure 5) reverses the relationship between
551 T and P on average over the summer.

552 In this analysis one should be reminded that the soil moisture-atmosphere interactions pathway
553 defined in Figure 2 also inherently includes the feedback of modified surface turbulent heat fluxes
554 on cloud cover and radiation. For instance, in the case of a negative precipitation anomaly and
555 subsequent soil moisture deficit, reduced evapotranspiration (which directly leads to higher surface
556 temperature) may also negatively impact cloud cover and thus enhance incoming shortwave
557 radiation, thereby further enhancing surface warming (Betts 2004, Ferranti and Viterbo 2006,
558 Davin et al. 2011, Gentine et al. 2013); it may even further reduce precipitation (e.g., Berg et al.
559 2013). The GLACE-CMIP5 experimental set-up does not allow for separating these feedbacks
560 from the direct impact of soil moisture on the surface energy budget and temperature. We note that
561 some models (ESM2M) show increased interannual variability of mean summertime cloud cover
562 between simulations REF and expA over some regions of negative T-P correlations, which
563 suggests that feedbacks of surface fluxes to cloud cover are at play over these regions; however
564 most models do not show such changes.

565 Overall, our analysis points to important uncertainties emerging at the seasonal-mean,
566 interannual timescale between climate models with respect to various functional relationships,
567 such as the control of soil moisture on evapotranspiration, the relationship of cloud cover with
568 radiation and precipitation, or the impact of surface radiation on temperature. These differences are
569 not unexpected, given that these emerging relationships are the result of small-scale
570 parameterization schemes, such as cloud, convection, radiation, soil hydrology, and boundary-
571 layer schemes. Through the interplay between these components, differences from the details of

572 these parameterizations grow and result in different behaviors at larger and longer spatio-temporal
573 scales. Consistent with our analysis, previous studies have noted, for instance, that climate models
574 exhibit different apparent sensitivities of surface temperature variability to processes such as
575 evapotranspiration and solar radiation (Lenderink et al. 2007, Fischer and Schar 2009). Such
576 uncertainties ultimately undermine our ability to use these models to analyze observed climate
577 phenomena such as T-P covariability: here, our multi-model analysis shows that model
578 uncertainties hinder a clear and quantitative understanding and attribution of observed T-P
579 correlations to particular processes, such as land-atmosphere interactions or cloud/radiative
580 processes. There is thus a need to better evaluate process-level, multivariate relationships in
581 climate models. We note, however, that while T-P correlations can readily be derived from
582 observations, more uncertainties and limitations affect observations of the relevant underlying
583 variables and their relationships at similar global and interannual scales (e.g., soil moisture, surface
584 fluxes, radiation). It is thus difficult to constrain climate models regarding these processes. We
585 note that recent studies indicate that climate models in CMIP5 tend to be too warm in summer over
586 land (Christensen and Boberg 2012, Mueller and Seneviratne 2014). While the comprehensive
587 causes of such biases are a subject of current investigation and may involve numerous physical
588 processes (e.g., Ma et al. 2014), one possibility is that they overestimate summertime drying, and
589 thus the subsequent feedback on surface temperature (Stegehuis et al. 2012). Locked in a dry and
590 warm soil moisture-limited regime, models may then overestimate soil moisture-atmosphere
591 interactions (Christensen and Boberg 2012). In contrast, some recent observational studies
592 emphasize the role of cloud cover in the variance of summer temperature (Tang et al. 2012, Tang
593 and Leng 2013). It is thus possible that models overestimate the contribution of soil moisture-
594 atmosphere interactions to the negative T-P correlations investigated in this study. Future

595 improvements in global land-atmosphere observational datasets, as well as point-wise land-
596 atmosphere model evaluation exercises, may help further constrain such model uncertainties.

597

598 **Conclusion**

599 Widespread negative correlations between summertime-mean temperatures and precipitation
600 have long been observed over land. Using simulations from the GLACE-CMIP5 multi-model
601 experiment with and without interactive soil moisture, we explored for the first time the
602 mechanisms responsible for such T-P covariability at the interannual time scale in a suite of
603 climate models. Our results generally confirm the interpretation of such correlations arising largely
604 through the direct control of soil moisture on surface heat flux partitioning: in all models soil
605 moisture-atmosphere interactions contribute largely to these correlations. However in some models
606 the association of cloud cover with precipitation on the one hand, and of solar radiation with
607 surface temperature on the other hand, appears sufficient to generate significant negative
608 correlations between temperature and precipitation, without feedbacks from the land surface. This
609 range of model behavior suggests that observed temperature-precipitation anti-correlations may
610 result from a combination of atmospheric and surface processes. Our results also underline the
611 uncertainties between models regarding cloud/radiative processes and their link to surface
612 temperature. Finally, we showed that on longer timescales, the negative correlation between
613 precipitation and temperature over land has implications for the projection of climate change
614 impacts on near surface climate: in all models, in regions of strong temperature-precipitation
615 coupling, long-term regional warming is modulated to a large extent by projected precipitation
616 changes. In most models this appears to be the result of soil moisture-atmosphere interactions. An
617 important issue in climate sciences is the response of the global hydrologic cycle to global
618 warming, in particular possible changes in precipitation patterns and amounts (e.g., Wentz et al.

619 2007). Our results demonstrate how regional-scale modifications to the water cycle can feed back
620 on surface temperature changes through soil moisture control on evapotranspiration. These results
621 imply that uncertainties in regional precipitation change, which are a well-documented issue of
622 climate model projections, in particular in the Tropics (e.g., Neelin et al. 2006, Knutti and
623 Sedlacek 2012), directly translate into uncertainties in temperature change. This arguably has
624 compounding effects on uncertainties associated with climate change impacts on natural and
625 human systems, but also suggests that reducing uncertainties in precipitation projections will help
626 reduce the uncertainties in projected regional temperature change. This also implies that the correct
627 representation of land surface hydrological processes in climate models is a key element to
628 providing improved and more robust regional projections of global climate change.

629

630

631 **Acknowledgments**

632 Alexis Berg was supported by National Science Foundation (NSF) grants AGS-1035968 and
633 AGS-1035843 and New Jersey Agricultural Experiment Station Hatch grant NJ07102, and is
634 currently supported by NSF Postdoctoral Fellowship AGS-1331375. S.I.S. acknowledges support
635 of the EU-FP7 EMBRACE project (European Commission's 7th Framework Programme, Grant
636 Agreement number 282672), and the GEWEX (World Climate Research Programme, WCRP) and
637 ILEAPS (Integrated Geosphere-Biosphere Programme, IGBP) projects, for the coordination and
638 realization of the GLACE-CMIP5 experiment. S.M. acknowledges support from the National
639 Oceanic and Atmospheric (US Department of Commerce) Grant NA08OAR4320752, US
640 Department of Agriculture Grant 2011-67003-30373, and the Carbon Mitigation Initiative at
641 Princeton University, sponsored by British Petroleum. Univ.Del., CMAP and GPCP datasets data
642 provided by the NOAA/OAR/ESRL PSD, Boulder, Colorado, USA, from their Web site at

643 <http://www.esrl.noaa.gov/psd/>. We thank Micah Wilhelm for his help with the GLACE-CMIP5
644 multi-model database.

645

646 REFERENCES

647 Adler, R. F., G. J. Gu, J. J. Wang, G. J. Huffman, S. Curtis, and D. Bolvin, 2008: Relationships between
648 global precipitation and surface temperature on interannual and longer timescales (1979–2006), *J. Geophys.*
649 *Res.-Atmos.*, **113**. D22104, doi:10.1029/2008JD010536.

650 Berg, A., K. Findell, B. Lintner, P. Gentine, C. Kerr, 2013: Precipitation Sensitivity to Surface Heat
651 Fluxes over North America in Reanalysis and Model Data. *J. Hydrometeor.*, **14**, 722–743.

652 Betts, A. K. . 2004: Understanding hydrometeorology using global models, *Bull. Am. Met. Soc.*, **85** (11),
653 1673–1688.

654 Christensen, J. H., and F. Boberg (2012), Temperature dependent climate projection deficiencies in
655 CMIP5 models, *Geophys. Res. Lett.*, **39**, L24705, doi:10.1029/2012GL053650.

656 Davin, E. L., R. Stöckli, E. B. Jaeger, S. Levis, and S. I. Seneviratne, 2011: COSMO-CLM²: a new
657 version of the COSMO-CLM model coupled to the Community Land Model. *Climate Dynamics*, **37**, 1889-
658 1907, doi: 10.1007/s00382-011-1019-z.

659 Déry, S. J., and E. F. Wood, 2005: Observed twentieth century land surface air temperature and
660 precipitation covariability, *Geophys. Res. Lett.*, **32**, L21414, doi:10.1029/2005GL024234.

661 Dirmeyer, P. A., 2011: The terrestrial segment of soil moisture-climate coupling. *Geophys. Res. Lett.*, **38**,
662 L16702, doi: 10.1029/2011GL048268.

663 Dirmeyer, P. A, B. A. Cash, J. L. Kinter III, C. Stan, T. Jung, L. Marx, P. Towers, N. Wedi, J. M. Adams,
664 E. L. Altshuler, B. Huang, E.K. Jin, and J. Manganello, 2012: Evidence for enhanced land-atmosphere
665 feedback in a warming climate. *J. Hydrometeor.*, **13**, 981-995.

666 Dirmeyer, P A., Y. Jin, B. Singh, and X. Yan, 2013: Trends in Land–Atmosphere Interactions from
667 CMIP5 Simulations. *J. Hydrometeor.*, **14**, 829–849.

668 Durre, I., J. M. Wallace, and D. P. Lettenmaier, 2000: Dependence of extreme daily maximum
669 temperatures on antecedent soil moisture in the contiguous United States during summer. *J. Climate*, **13**,
670 2641–2651.

671 Entekhabi, D., I. Rodríguez-Iturbe, and R. L. Bras, 1992: Variability in Large-Scale Water-Balance with
672 Land Surface Atmosphere Interaction. *Journal of Climate*, **5**(8), 798–813.

673 Ferranti, L., and P. Viterbo, 2006: Sensitivity to soil water initial conditions. *J. Climate*, **19**, 3659–3680.
674

675 Fischer, E. M., S. I. Seneviratne, D. Luthi, and C. Schär , 2007: Contribution of land-atmosphere coupling
676 to recent European summer heat waves, *Geophys. Res. Lett.*, **34**, L06707, doi:10.1029/2006GL029068.

677 Fischer, E., C. Schar, 2009: Future changes in daily summer temperature variability: driving processes
678 and role for temperature extremes, *Climate Dynamics*, **33**(7-8), 917-935, doi: 10.1007/s00382-008-0473-8.

679 Gentine, P., A. A. Holtslag, F D'Andrea, and M. Ek, 2013: Surface and atmospheric controls on the onset
680 of moist convection over land. *J. Hydrometeor.*, **14**(5).

681 Guo, Z., and co-authors, 2006: GLACE: The Global Land-Atmosphere Coupling Experiment. 2.
682 Analysis. *J. Hydrometeor.*, **7**, 611-625, doi: 10.1175/JHM511.1.

683 Haarsma, R.J., F. Selten, B. van den Huk, W. Hazeleger, and X. L. Wang, 2009: Drier Mediterranean
684 soils due to greenhouse warming bring easterly winds over summertime central Europe. *Geophys. Res.*
685 *Lett.*, **36**, L04705.

686 Hirschi, M., et al., 2011: Observational evidence for soil-moisture impact on hot extremes in southeastern
687 Europe, *Nat. Geosci.*, **4**, 17.

688 Jung, M., and Coauthors, 2010: Recent decline in the global land evapotranspiration trend due to limited
689 moisture supply. *Nature*, **467**, 951–954.

690

691 Knutti, R., and J. Sedláček, 2012: Robustness and uncertainties in the new CMIP5 climate model
692 projections. *Nat. Climate Change*, **3**(4), 369-373.

693 Koster, R.D. et al. 2004: Regions of strong coupling between soil moisture and precipitation. *Science*,
694 **305**, 1138-1140.

695 Koster, R.D., et al. 2006: GLACE: The Global Land-Atmosphere Coupling Experiment. Part I: Overview.
696 *J. Hydrometeor.*, **7**, 590-610.

697 Koster, R.D., S.D. Schubert, and M.J. Suarez, 2009a: Analyzing the concurrence of meteorological
698 droughts and warm periods, with implications for the determination of evaporative regime. *J. Climate*, **22**,
699 3331-3341.

700 Koster, R. D., Z. Guo, R. Yang, P. A. Dirmeyer, K. Mitchell, K., and M. J. Puma, 2009b: On the Nature
701 of Soil Moisture in Land Surface Models. *J. Climate*, **22**(16), 4322–4335.

702 Koster, R.D., S. Mahanama, T. J. Yamada, G. Balsamo, M. Boisserie, P. A. Dirmeyer, F. Doblas-Reyes,
703 C. T. Gordon, Z. Guo, J. H. Jeong, D. Lawrence, Z. Li, L. Luo, S. Malyshev, W. Merryfield, S. I.
704 Seneviratne, T. Stanelle, B. van den Hurk, F. Vitart, and E.F. Wood, 2010: The contribution of land
705 initialization to subseasonal forecast skill: First results from the GLACE-2 Project. *Geophys. Res. Lett.*, **37**,
706 L02402.

707 Krakauer, N., B. Cook, and M. Puma, 2010: Contribution of soil moisture feedback to hydroclimatic
708 variability. *Hydrol. Earth Syst. Sci.*, **14**, 505–520.

709 Lenderink, G., A. van Ulden, B. van den Hurk and E. van Meijgaard, 2007: Summertime inter-annual
710 temperature variability in an ensemble of regional model simulations: analysis of the surface energy budget.
711 *Climatic Change*, **81**, 233-247.

712 Livezey, R. E. and Chen, W. Y., 1983: Statistical field significance and its determination by Monte Carlo
713 techniques. *Monthly Weather Review*, 111(1), 46-59.

714 Ma, H.-Y., and Coauthors, 2014: On the Correspondence between Mean Forecast Errors and Climate
715 Errors in CMIP5 Models. *J. Climate*, 27, 1781–1798.

716 Madden, R. A., and J. Williams, 1978: The correlation between temperature and precipitation in the
717 United States and Europe. *Mon. Weather Rev.*, **106**, 142–147.

718 Miralles, D. G.; M. J. van den Berg, A. J. Teuling, and R. A. M. de Jeu, 2012: Soil moisture-temperature
719 coupling: A multiscale observational analysis. *Geophys. Res. Lett.*, **39**, L21707

720 Mueller, B., and S. I. Seneviratne, 2012: Hot days induced by precipitation deficits at the global scale.
721 *Proc. Natl. Acad. Sci. U.S.A.*, **109** (31), 12398-12403.

722 Mueller, B., and S. I. Seneviratne, 2014: Systematic land climate and evapotranspiration biases in CMIP5
723 simulations. *Geophys. Res. Lett.*, **41**, doi:10.1002/2013GL058055.

724 Muller, C. J., L. E. Back, P. A. O’Gorman, and K. E. Emanuel, 2009: A model for the relationship
725 between tropical precipitation and column water vapor. *Geophys. Res. Lett.*, **36**, L16804.
726 doi:10.1029/2009GL039667.

727 Muller, C. J., P. A. O’Gorman, and L. E. Back, 2011: Intensification of Precipitation Extremes with
728 Warming in a Cloud-Resolving Model. *J Climate*, **24**(11), 2784–2800. doi:10.1175/2011JCLI3876.1.

729 Neelin, J. D., M. Munnich, H. Su, J. E. Meyerson, and C. E. Holloway, 2006: Tropical drying trends in
730 global warming models and observations. *Proc. Natl. Acad. Sci. U. S. A.*, **103**(16), 6110–6115.

731 Portmann, R. W., S. Solomon, and G. C. Hegerl, 2009: Spatial and seasonal patterns in climate change,
732 temperatures, and precipitation across the United States. *Proc. Natl. Acad. Sci. U. S. A.*, **106**, 7324–7329.

733 Quesada, B., R. Vautard, P. Yiou, M. Hirschi, and S. I. Seneviratne, 2012: Asymmetric European summer
734 heat predictability from wet and dry southern winters and springs. *Nat. Climate Change*, **2**, 736–741.

735 Rebetez, M., 1996: Seasonal relationship between temperature, precipitation and snow cover in a moun-
736 tainous region. *Theor. Appl. Climatol.*, **54**(3–4), 99–106.

737 Rusticucci, M., and O. Penalba, 2000: Interdecadal changes in the precipitation seasonal cycle over
738 southern South America and their relationship with surface temperature. *Climate Res.*, **16**, 1–15.

739 Seneviratne, S. I., D. Lüthi, M. Litschi, and C. Schär, 2006: Land-atmosphere coupling and climate
740 change in Europe. *Nature*, **443**, 205–209.

741 Seneviratne, S. I., T. Corti, E. L. Davin, M. Hirschi, E. B. Jaeger, I. Lehner, B. Orlowsky, and A. J.
742 Teuling, 2010: Investigating soil moisture-climate interactions in a changing climate: A review. *Earth-Sci*
743 *Rev.*, **99**, 3-4, 125-161, doi:10.1016/j.earscirev.2010.02.004.

744 Seneviratne, S. I., M. Wilhelm, T. Stanelle, B.J.J.M. van den Hurk, S. Hagemann, A. Berg, F. Cheruy, M.
745 E. Higgins, A. Meier, V. Brovkin, M. Claussen, A. Ducharne, J.-L. Dufresne, K. L. Findell, J. Ghattas, D.
746 M. Lawrence, S. Malyshev, M. Rummukainen, and B. Smith, 2013: Impact of soil moisture-climate
747 feedbacks on CMIP5 projections: First results from the GLACE-CMIP5 experiment. *Geophys. Res. Lett.*,
748 **40**, 5212-5217, doi:10.1002/grl.50956.

749 Shinoda, M., and Y. Yamaguchi, 2003: Influence of soil moisture anomaly on temperature in the Sahel: A
750 comparison between wet and dry decades. *J. Hydrometeor.*, **4**, 437–447.

751 Stegehuis, A., R. Vautard, P. Ciais, R. Teuling, M. Jung, and P. Yiou, 2013: Summer temperatures in
752 Europe and land heat fluxes in observation-based data and regional climate model simulations. *Climate*
753 *Dynamics*, **41**, 455-477.

754 Sutton RT, B.-W. Dong, and J. M. Gregory, 2007: Land/sea warming ratio in response to climate change:
755 IPCC AR4 model results and comparison with observations. *Geophys. Res. Lett.*, **34**, L02701

756 Tang, Q., G. Leng, and P. Y. Groisman, 2012: European Hot Summers Associated with a Reduction of
757 Cloudiness. *J. Climate*, **25**, 3637–3644.

758 Tang, Q., and G. Leng, 2013: Changes in Cloud Cover, Precipitation, and Summer Temperature in North
759 America from 1982 to 2009. *J. Climate*, **26**, 1733–1744.

760 Teuling, A. J., and Coauthors, 2009: A regional perspective on trends in continental
761 evaporation. *Geophys. Res. Lett.*, **36**, L02404, doi:10.1029/2008GL036584.

762 Trenberth, K. E., and D. J. Shea, 2005: Relationships between precipitation and surface temperature.
763 *Geophys. Res. Lett.*, **32**, L14703, doi:10.1029/2005GL022760.

764 Tout, D. G., 1987: Precipitation-temperature relation- ship in England and Wales summers. *Int. J. Clima-*
765 *tol.*, **7**(2), 181–184.

766 Vautard, R., P. Yiou, F. D'Andrea, N. de Noblet, N. Viovy, C. Cassou, J. Polcher, P. Ciais, M. Kageyama,
767 and Y. Fan, 2007: Summertime European heat and drought waves induced by wintertime Mediterranean
768 rainfall deficit. *Geophys. Res. Lett.*, **34**, L07711, doi:10.1029/2006GL028001.

769 Wentz, F. J., L. Ricciardulli, K. Hilburn, and C. Mears, 2007: How much more rain will global warming
770 bring? *Science*, **317**, 233–235.

771 Wu, R. G., J. P. Chen, and Z. P. Wen, 2013: Precipitation–surface temperature relationship in the IPCC
772 CMIP5 Models. *Adv. Atmos. Sci.*, **30**(3), 766–778, doi: 10.1007/s00376-012-2130-8.

773 Zampieri, M., F. D'Andrea, R. Vautard, P. Ciais, N. de Noblet-Ducoudré, and P. Yiou, 2009: Hot
774 European summers and the role of soil moisture in the propagation of Mediterranean drought. *J Climate*,
775 **22**(18), 4747–4758.

776 Zhao, W., and M. A. K. Khalil, 1993: The relationship between precipitation and temperature over the
777 contiguous United States. *J. Climate*, **6**, 1232–1236.

778

779 Fig.1: Point-wise, zero-lag correlations of summertime-mean temperature (T) against
780 precipitation (P), using different datasets. CRU: Climatic Research Unit (CRU) Time-Series (TS)
781 Version 3.21; UoD: University of Delaware Monthly Temperature and Precipitation dataset V3.01;
782 NASA: NASA Goddard Institute for Space Studies GISTEMP Surface Temperature Analysis;
783 ERAI: ERA-Interim reanalysis; GPCP: Global Precipitation Climatology Project monthly
784 precipitation dataset V.2.2; CMAP: CPC Merged Analysis of Precipitation V.1201. Top two plots
785 (CRU and UoD) use full record lengths, at original resolution ($0.5^{\circ}\times 0.5^{\circ}$). All other plots use data
786 regridded on a common $2.5^{\circ}\times 2.5^{\circ}$ grid (over 1979-2008). Increments on the color scale correspond
787 to the 10%, 5%, 1%, 0.1% levels of correlation significance (for different record lengths); non-
788 significant correlations (at 10%) are whited out. Antarctica and Greenland are removed from all
789 datasets. Numbers within plots indicate, on the bottom-center: the land percentage with significant
790 (5%) T-P correlations (in blue, negative correlations only, in red, positive correlations); on the
791 bottom-right: the field-significance threshold, as estimated by a Monte-Carlo procedure in which
792 yearly maps of T and P were randomly shuffled 1000 times; the threshold used is the 95% quantile
793 of the corresponding 1000-member distribution of area percentage with significant (5%)
794 correlations (e.g., Livezey and Chen 1983). The dashed equatorial line separates JJA (June-July-
795 August) means which are used for the Northern Hemisphere and DJF (December-January-
796 February) means used for the Southern Hemisphere.

797 Fig.2: Simplified representation of two pathways through which correlations between seasonal
798 mean temperature and precipitation can occur in summer: red, atmospheric processes; blue, land-
799 atmosphere interactions. Note that in the interest of clarity, not all physical relationships are
800 depicted here (e.g., impacts of temperature on soil moisture, feedbacks of surface fluxes to cloud
801 cover, etc., are not represented).

802 Fig.3: As in Figure 1, but for GLACE-CMIP5 models over 1971-2000, in simulation REF (**a**)
803 and simulation expA (**b**). Color key corresponds to the 10%, 5%, 1%, 0.1% levels of correlation
804 significance.

805 Fig.4: In simulation REF (red) and expA (blue), sum of the grid cell areas with significant
806 negative T-P correlations (at the 5% level, i.e. $r=0.36$), weighted by the T-P correlation values on
807 these grid cells.

808 Fig.5: (**a**) Correlation between summertime-mean total soil moisture and evapotranspiration
809 ($\text{cor}(\text{SM},\text{ET})$); (**b**) correlation between summertime-mean temperature and evapotranspiration
810 ($\text{cor}(\text{ET},\text{T})$); (**c**) correlation between summertime-mean incoming shortwave radiation and
811 evapotranspiration ($\text{cor}(\text{Rs},\text{ET})$), over 1971-2000, in simulation REF, for the different models.
812 Color key corresponds to the 10%, 5%, 1%, 0.1% levels of correlation significance.

813 Figure 6: Correlation between summertime-mean evapotranspiration and incoming shortwave
814 radiation, over 1971-2000, for the different models in expA. Color key corresponds to the 10%,
815 5%, 1%, 0.1% levels of correlation significance.

816 Fig.7: Correlation in simulation expA between summertime-mean incoming shortwave radiation
817 and: (**a**) precipitation, and (**b**) temperature, over 1971-2000. (**c**) is the same as Figure 3b, i.e. T-P
818 correlations in simulation expA, with black contours indicating where the correlations between
819 summertime-mean temperature and radiation (seen in **b**) are significantly positive while the
820 correlations between summertime-mean precipitation and radiation (seen in **a**) are significantly
821 negative. Background land maps have been grayed (and interior borders were suppressed) in (**c**) to
822 facilitate readability. Color key corresponds to the 10%, 5%, 1%, 0.1% levels of correlation
823 significance.

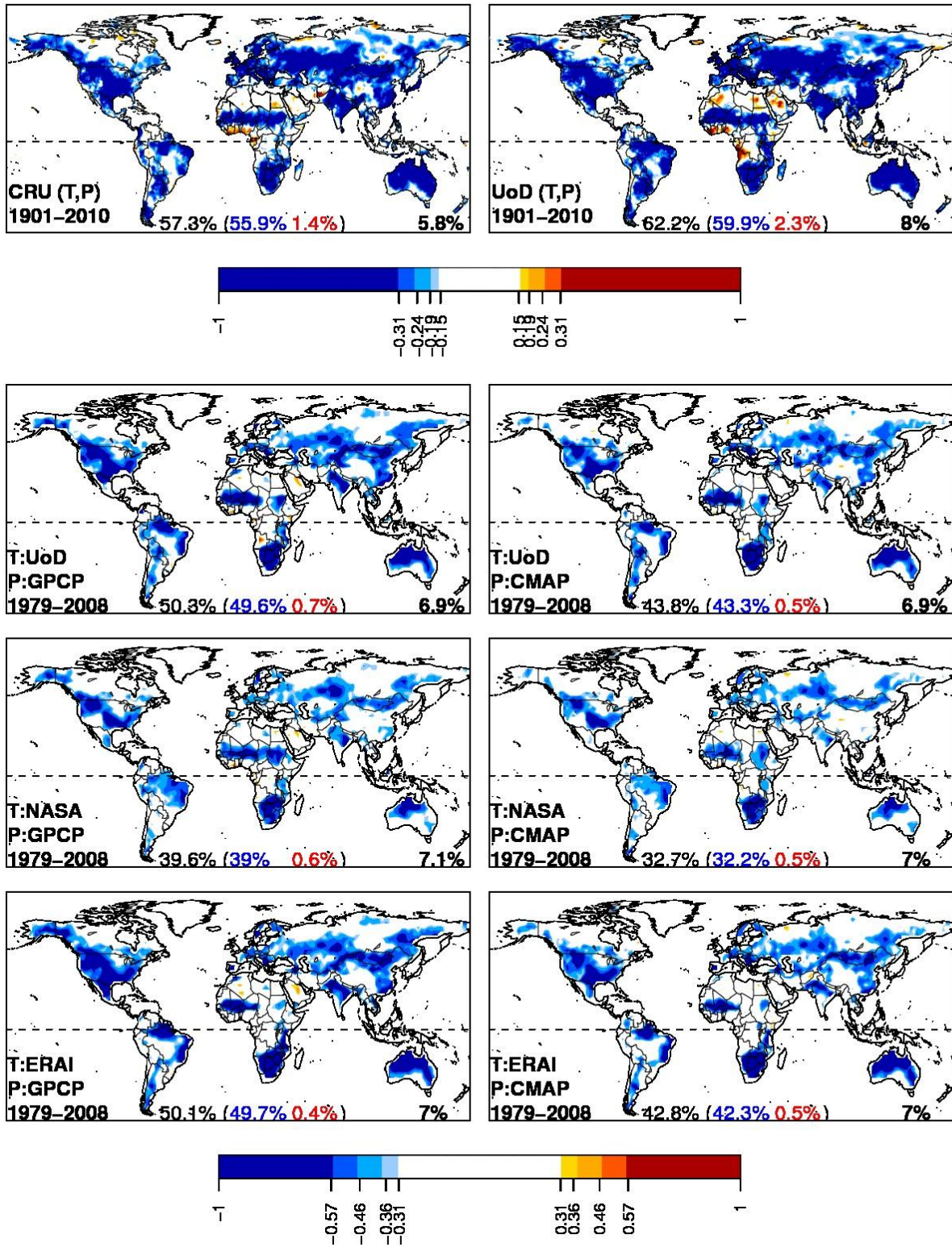
824 Fig.8: **(a)** Correlation between summertime-mean temperature and precipitation, in simulation
825 REF, binned as a function of correlations between soil moisture and evapotranspiration
826 ($\text{cor}(\text{SM},\text{ET})$, x-axis) and between evapotranspiration and temperature ($\text{cor}(\text{ET},\text{T})$, y-axis), for the
827 different models, over 1971-2000, over land. Blue and red contours indicate, respectively, negative
828 and positive temperature-precipitation correlations significant at the 5% level ($r=0.36$); **(b)**
829 percentage of total number of land pixels in each model that fall in each $\text{cor}(\text{SM},\text{E})$ - $\text{cor}(\text{E},\text{T})$ bin.

830 Fig.9: Share of the land surface area (in %) where T-P, SM-ET and ET-T correlations become
831 significantly more positive (positive bars) or significantly more negative (negative bars) between
832 1971-2000 and 2071-2100 (the difference being represented is future minus present) in different
833 models in REF.

834 Fig.10: **(a)** Mean summer T change between 1971-2000 and 2071-2100, in K, in simulation
835 REF; **(b)** mean summer T change between 1971-2000 and 2071-2100 from **(a)** (color key in K)
836 binned along correlations between present-time (1971-2000) summertime-mean T and P ($\text{cor}(\text{T},\text{P})$,
837 x-axis) and mean summertime P change between 1971-2000 and 2071-2100 (y-axis, in mm/d),
838 over land pixels only.

839 Fig.11: Same as Figure 10, for simulation expA. Note that temperature changes over the oceans
840 in **(a)** are the same as in Figure 10 in simulation REF, since similar sea surface temperatures were
841 prescribed in both experiments.

842

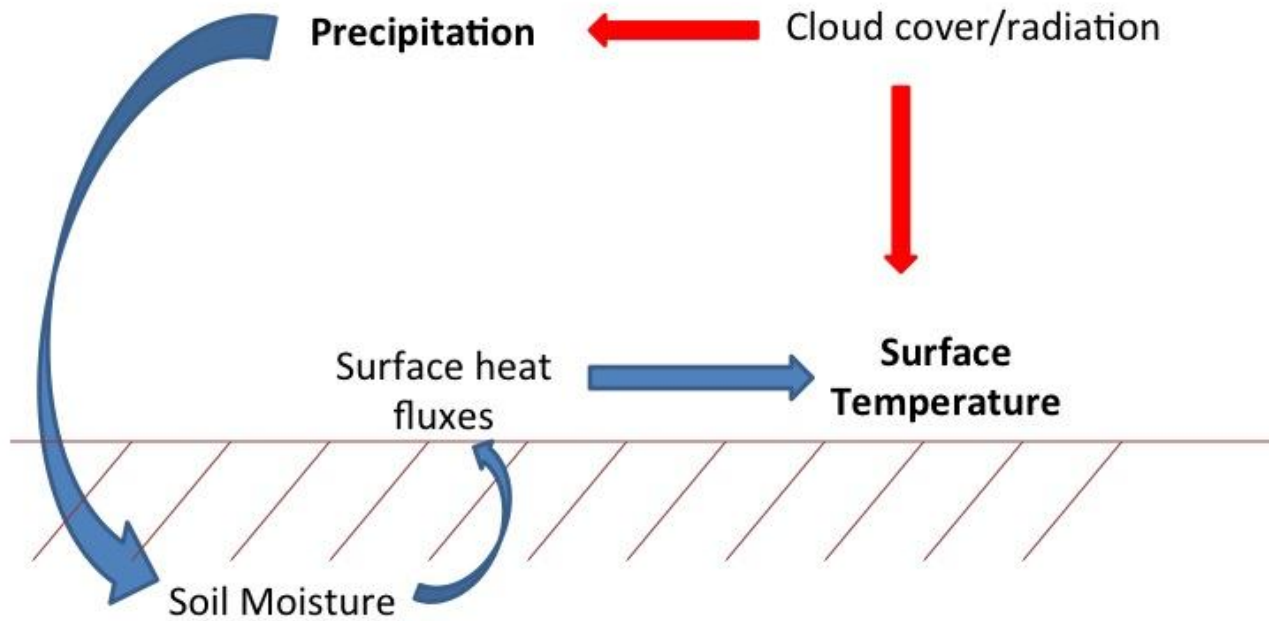


843

844 Fig.1: Point-wise, zero-lag correlations of summertime-mean temperature (T) against
 845 precipitation (P), using different datasets. CRU: Climatic Research Unit (CRU) Time-Series (TS)
 846 Version 3.21; UoD: University of Delaware Monthly Temperature and Precipitation dataset V3.01;

847 NASA: NASA Goddard Institute for Space Studies GISTEMP Surface Temperature Analysis;
848 ERAI: ERA-Interim reanalysis; GPCP: Global Precipitation Climatology Project monthly
849 precipitation dataset V.2.2; CMAP: CPC Merged Analysis of Precipitation V.1201. Top two plots
850 (CRU and UoD) use full record lengths, at original resolution ($0.5^\circ \times 0.5^\circ$). All other plots use data
851 regrided on a common $2.5^\circ \times 2.5^\circ$ grid (over 1979-2008). Increments on the color scale correspond
852 to the 10%, 5%, 1%, 0.1% levels of correlation significance (for different record lengths); non-
853 significant correlations (at 10%) are whited out. Antarctica and Greenland are removed from all
854 datasets. Numbers within plots indicate, on the bottom-center: the land percentage with significant
855 (5%) T-P correlations (in blue, negative correlations only, in red, positive correlations); on the
856 bottom-right: the field-significance threshold, as estimated by a Monte-Carlo procedure in which
857 yearly maps of T and P were randomly shuffled 1000 times; the threshold used is the 95% quantile
858 of the corresponding 1000-member distribution of area percentage with significant (5%)
859 correlations (e.g., Livezey and Chen 1983). The dashed equatorial line separates JJA (June-July-
860 August) means which are used for the Northern Hemisphere and DJF (December-January-
861 February) means used for the Southern Hemisphere.

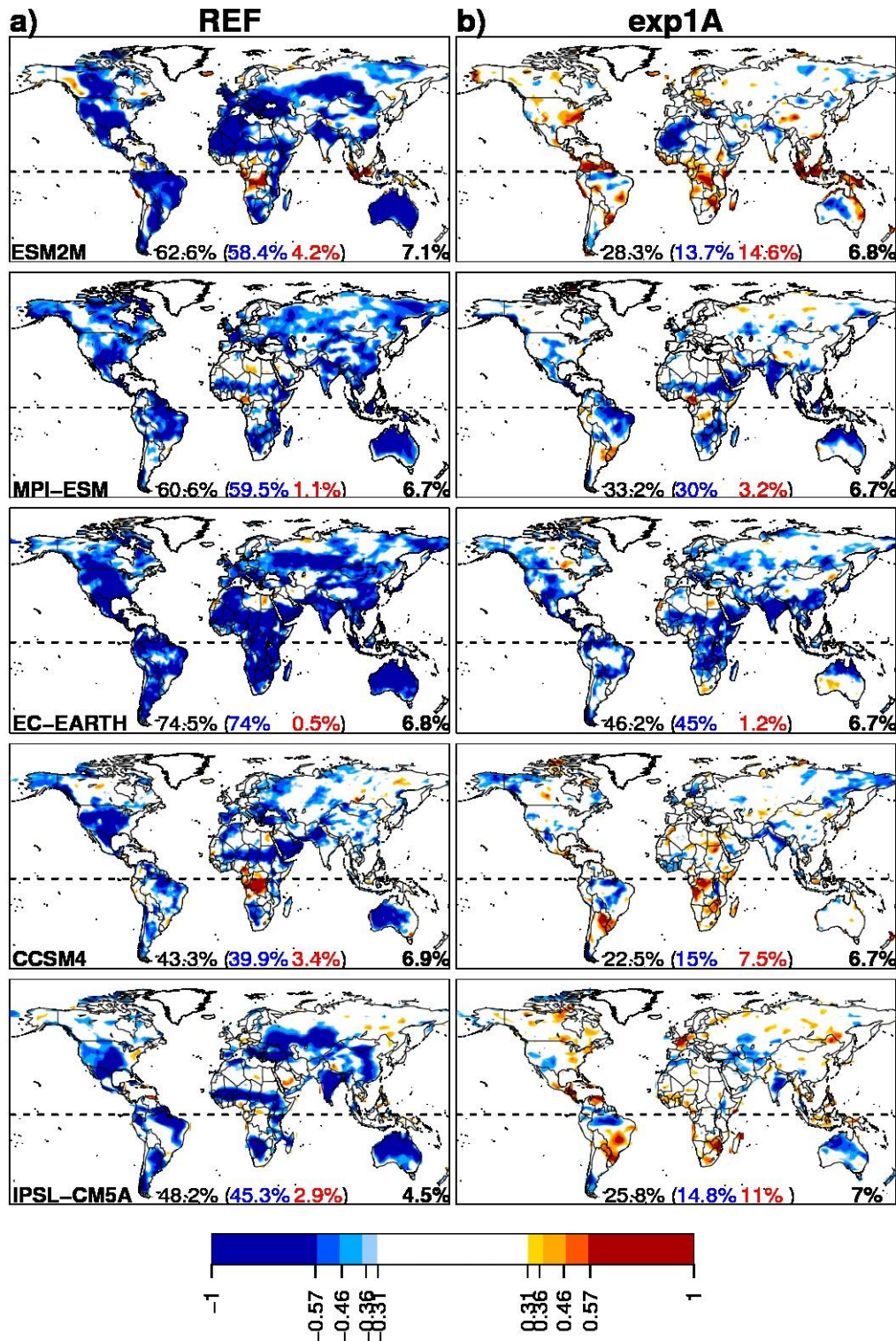
862



863

864 Fig.2: Simplified representation of two pathways through which correlations between seasonal
 865 mean temperature and precipitation can occur in summer: red, atmospheric processes; blue, land-
 866 atmosphere interactions. Note that in the interest of clarity, not all physical relationships are
 867 depicted here (e.g., impacts of temperature on soil moisture, feedbacks of surface fluxes to cloud
 868 cover, etc., are not represented).

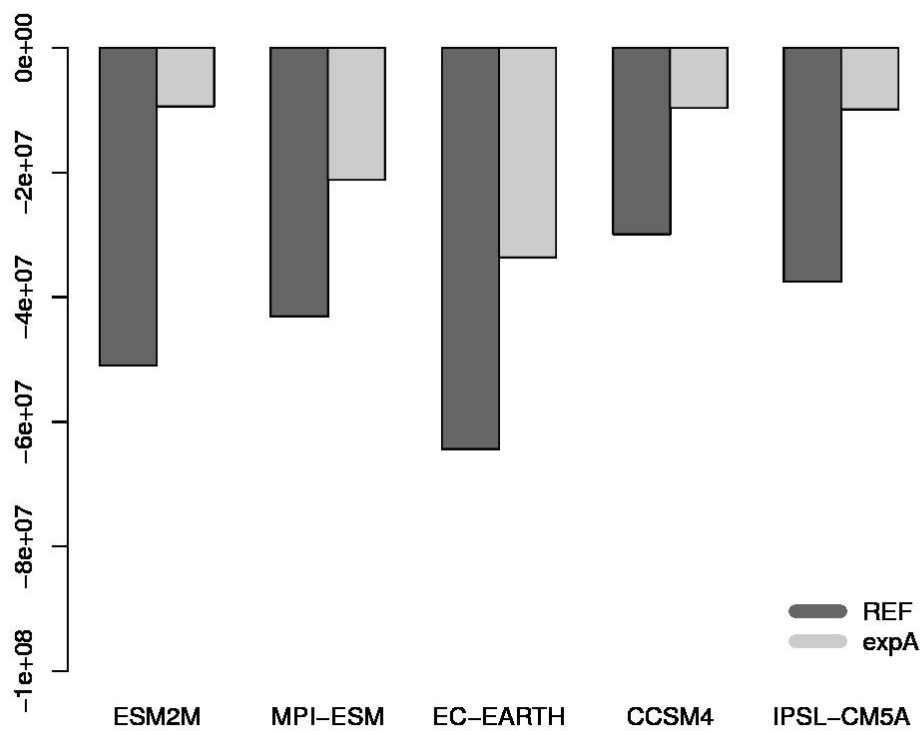
869



870

871 Fig.3: As in Figure 1, but for GLACE-CMIP5 models over 1971-2000, in simulation REF (a)
 872 and simulation expA (b). Color key corresponds to the 10%, 5%, 1%, 0.1% levels of correlation
 873 significance.

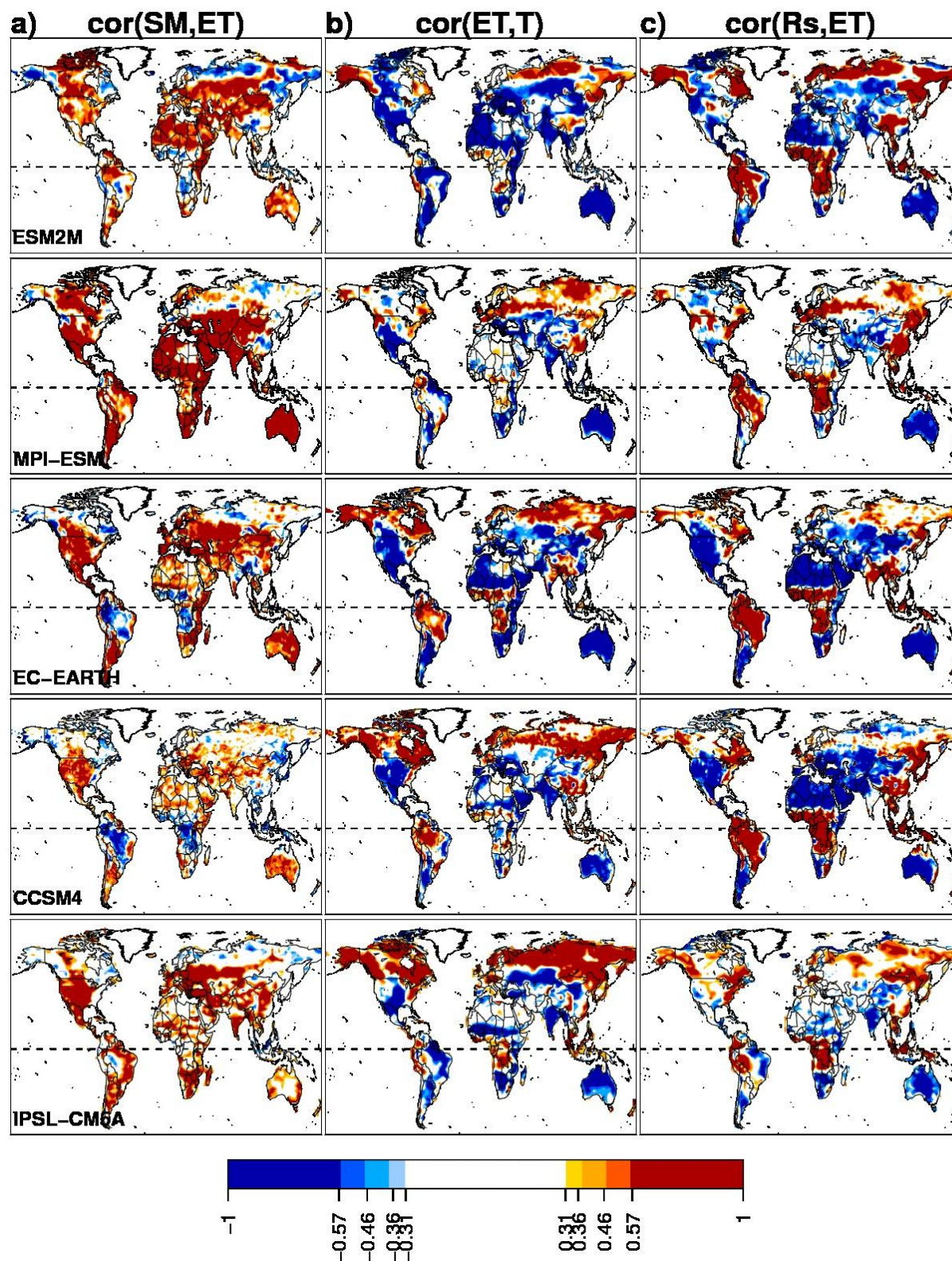
874



875

876 Fig.4: In simulation REF (red) and expA (blue), sum of the grid cell areas with significant
 877 negative T-P correlations (at the 5% level, i.e. $r=0.36$), weighted by the T-P correlation values on
 878 these grid cells.

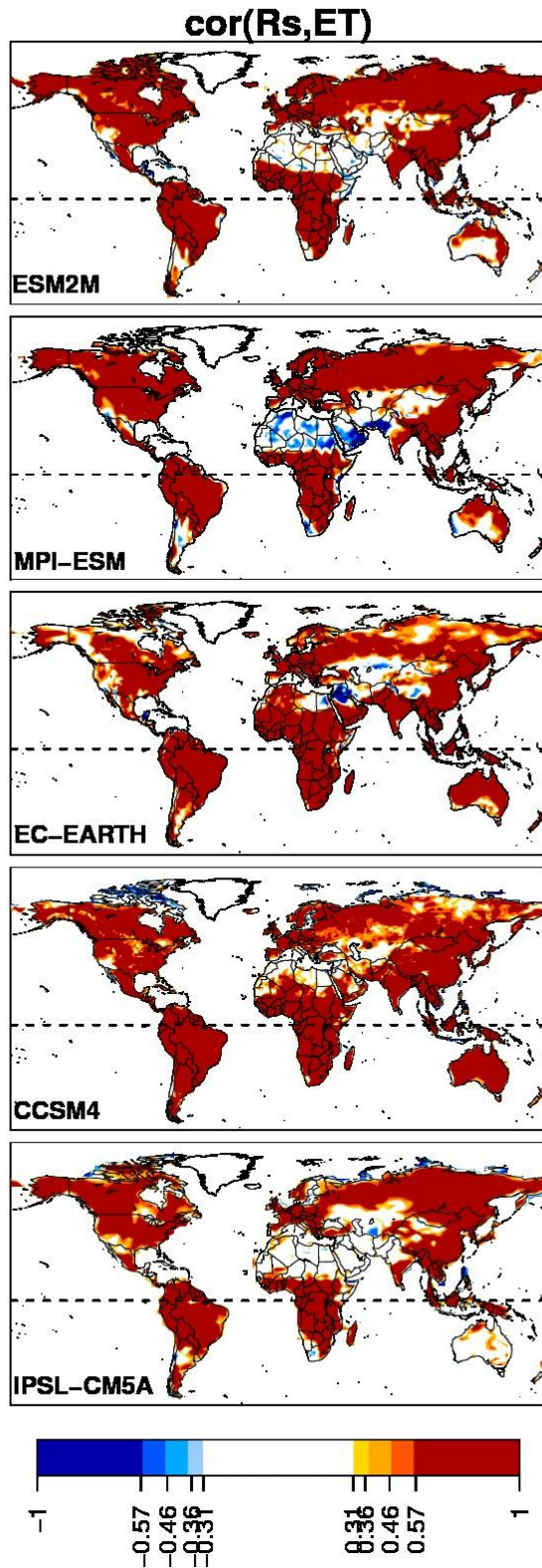
879



880

881 Fig.5: (a) Correlation between summertime-mean total soil moisture and evapotranspiration
 882 ($\text{cor}(\text{SM}, \text{ET})$); (b) correlation between summertime-mean temperature and evapotranspiration
 883 ($\text{cor}(\text{ET}, \text{T})$); (c) correlation between summertime-mean incoming shortwave radiation and

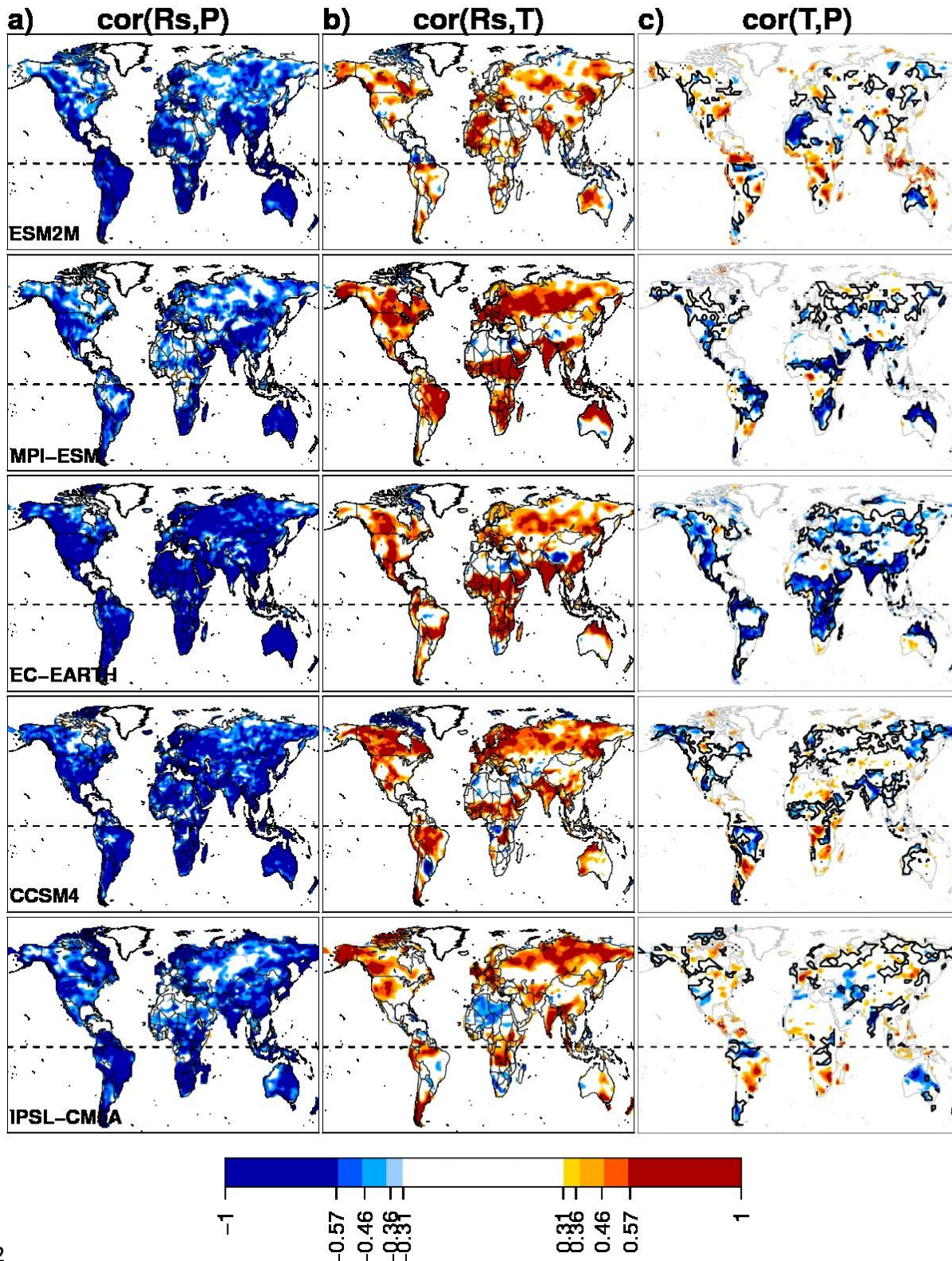
884 evapotranspiration ($\text{cor}(R_s, ET)$), over 1971-2000, in simulation REF, for the different models.
885 Color key corresponds to the 10%, 5%, 1%, 0.1% levels of correlation significance.
886



887

888 Figure 6: Correlation between summertime-mean evapotranspiration and incoming shortwave
 889 radiation, over 1971-2000, for the different models in expA. Color key corresponds to the 10%,
 890 5%, 1%, 0.1% levels of correlation significance.

891

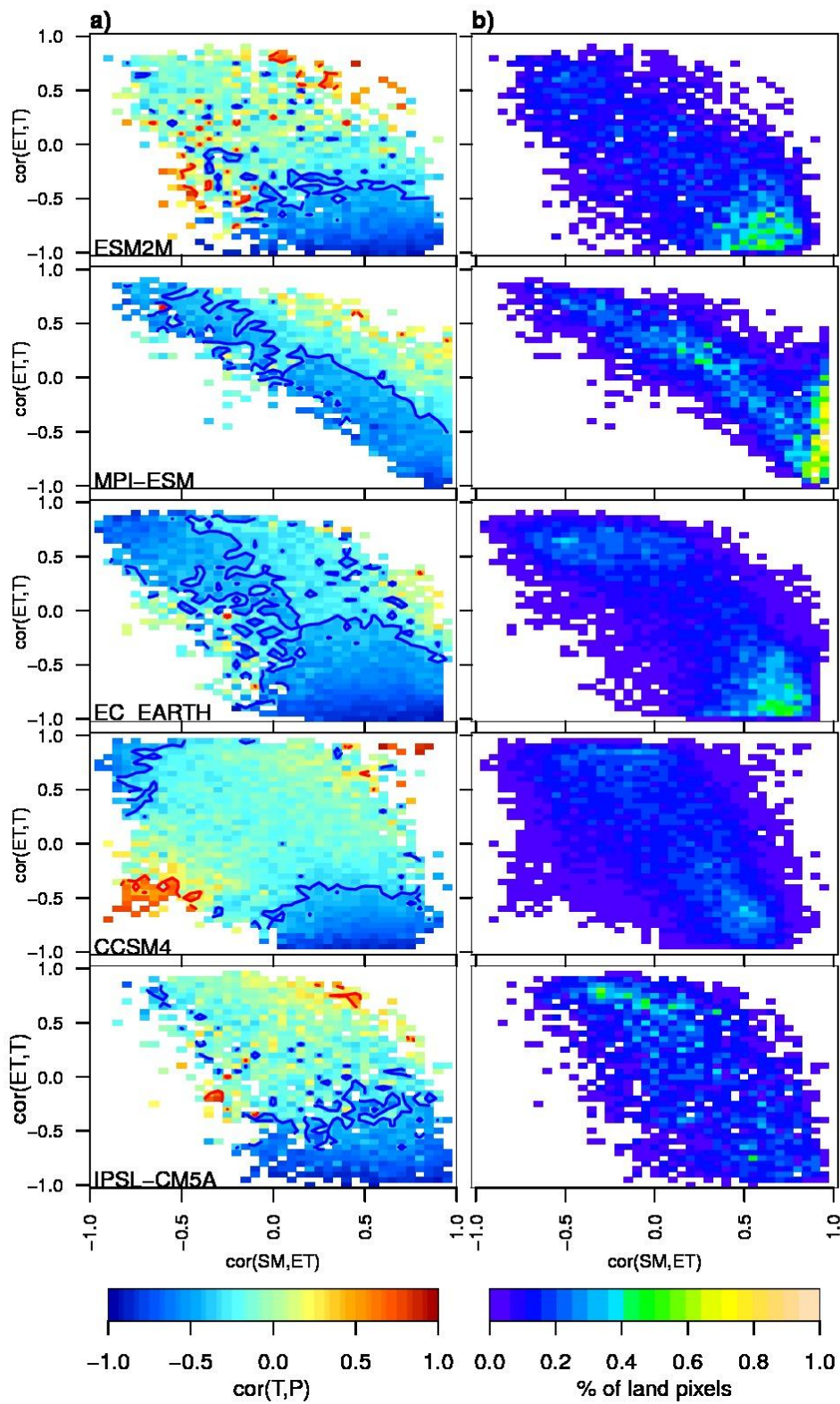


892

893 Fig. 7: Correlation in simulation expA between summertime-mean incoming shortwave radiation
 894 and: (a) precipitation, and (b) temperature, over 1971-2000. (c) is the same as Figure 3b, i.e. T-P
 895 correlations in simulation expA, with black contours indicating where the correlations between

896 summertime-mean temperature and radiation (seen in **b**) are significantly positive while the
897 correlations between summertime-mean precipitation and radiation (seen in **a**) are significantly
898 negative. Background land maps have been grayed gray (and interior borders were suppressed) in
899 (c) to facilitate readability. Color key corresponds to the 10%, 5%, 1%, 0.1% levels of correlation
900 significance.

901

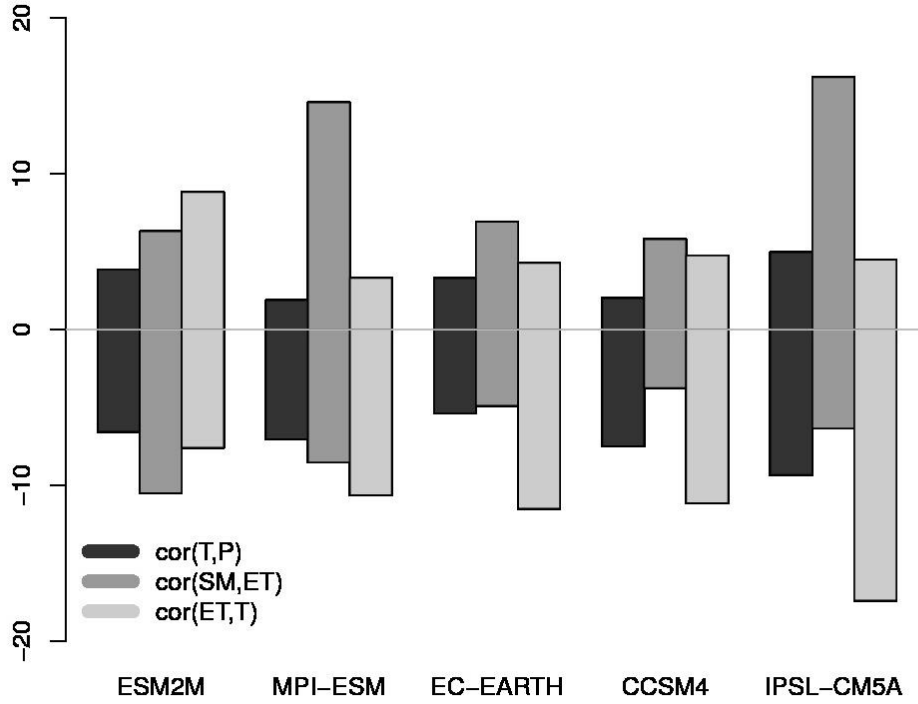


902

903 Fig.8: (a) Correlation between summertime-mean temperature and precipitation, in simulation
 904 REF, binned as a function of correlations between soil moisture and evapotranspiration
 905 ($\text{cor}(SM, ET)$, x-axis) and between evapotranspiration and temperature ($\text{cor}(ET, T)$, y-axis), for the

906 different models, over 1971-2000, over land. Blue and red contours indicate, respectively, negative
907 and positive temperature-precipitation correlations significant at the 5% level ($r=0.36$); **(b)**
908 percentage of total number of land pixels in each model that fall in each $\text{cor}(\text{SM},\text{E})$ - (corE,T) bin.

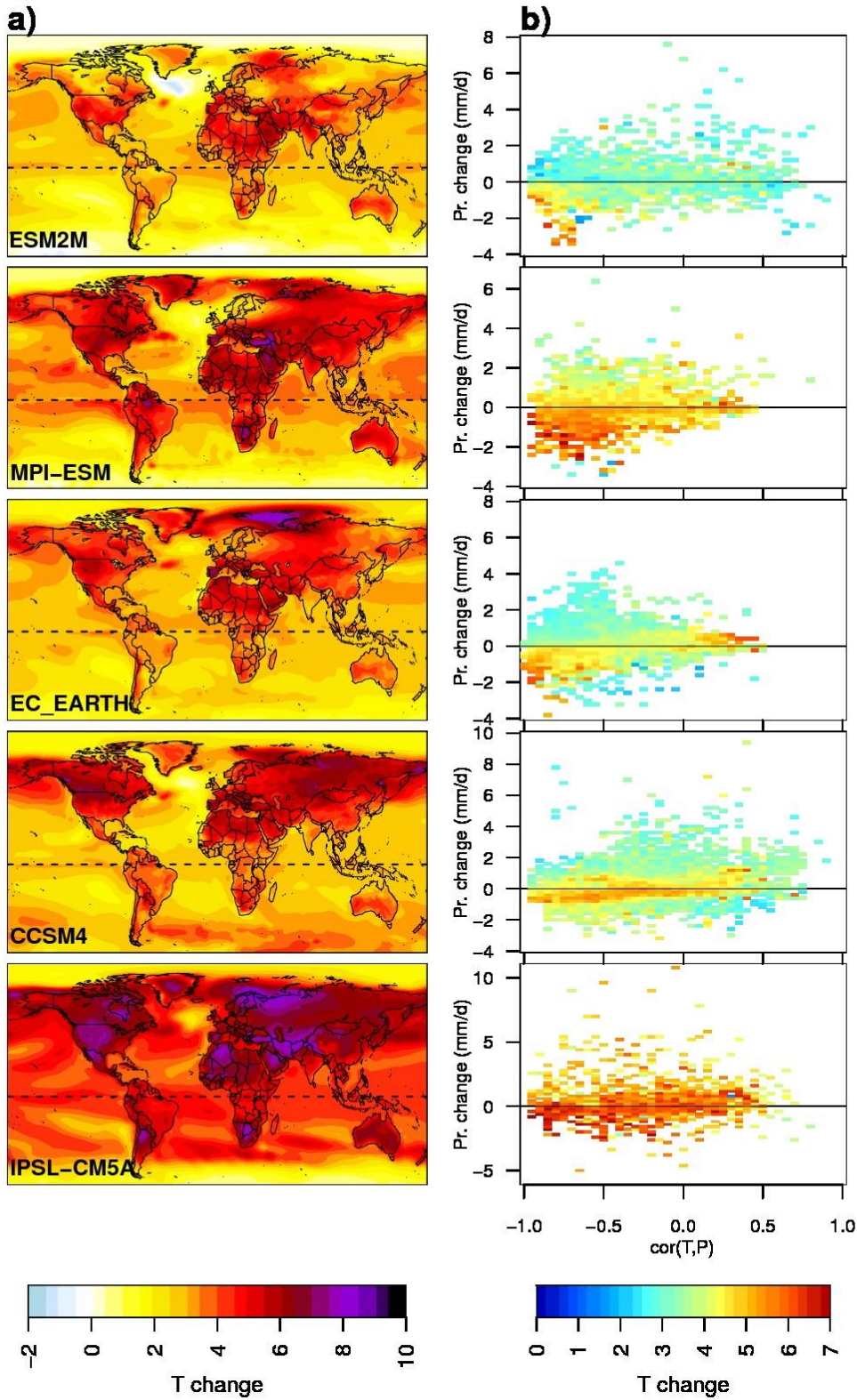
909



910

911 Fig.9: Share of the land surface area (in %) where T-P, SM-ET and ET-T correlations become
 912 significantly more positive (positive bars) or significantly more negative (negative bars) between
 913 1971-2000 and 2071-2100 (the difference being represented is future minus present) in different
 914 models in REF.

915

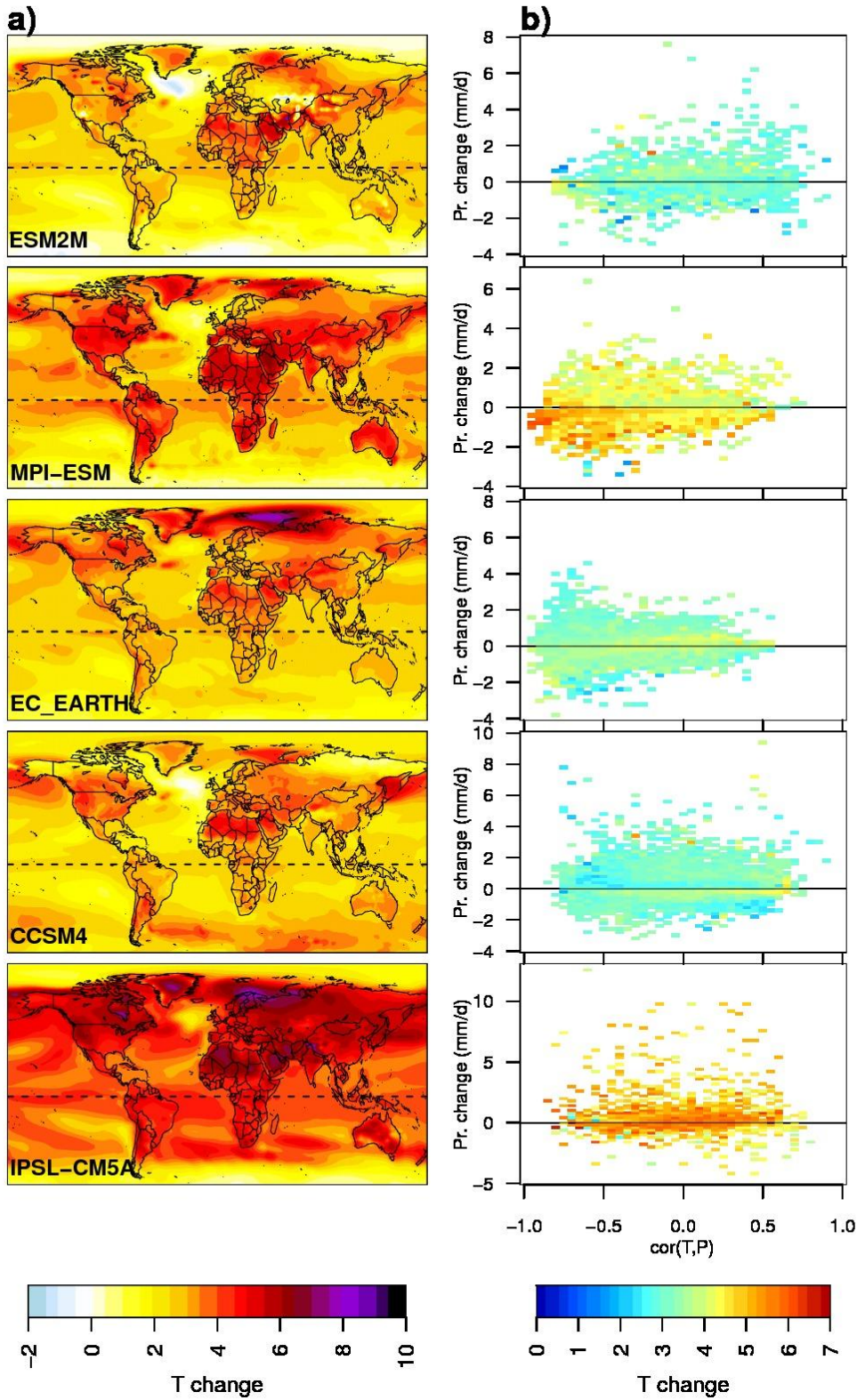


916

917 Fig.10: (a) Mean summer T change between 1971-2000 and 2071-2100, in K, in simulation
 918 REF; (b) mean summer T change between 1971-2000 and 2071-2100 from (a) (color key in K)
 919 binned along correlations between present-time (1971-2000) summertime-mean T and P ($cor(T,P)$),

920 x-axis) and mean summertime P change between 1971-2000 and 2071-2100 (y-axis, in mm/d),
921 over land pixels only.

922



923

924 Fig.11: Same as Figure 10, for simulation expA. Note that temperature changes over the oceans
 925 in (a) are the same as in Figure 10 in simulation REF, since similar sea surface temperatures were
 926 prescribed in both experiments.

Supplemental Material

[Click here to download Supplemental Material: Suppl_Mat_Berg_et_al.pdf](#)

Figure 1

[Click here to download Non-Rendered Figure: figure1_revised.eps](#)

Figure 2

[Click here to download Non-Rendered Figure: Figure2_revised.jpg](#)

Figure 3

[Click here to download Non-Rendered Figure: figure3_revised.eps](#)

Figure 4

[Click here to download Non-Rendered Figure: figure4_revised.eps](#)

Figure 5

[Click here to download Non-Rendered Figure: figure5_revised.eps](#)

Figure 6

[Click here to download Non-Rendered Figure: figure6_revised.eps](#)

Figure 7

[Click here to download Non-Rendered Figure: figure7_revised.eps](#)

Figure 8

[Click here to download Non-Rendered Figure: figure8_revised.eps](#)

Figure 9

[Click here to download Non-Rendered Figure: figure9_revised.eps](#)

Figure 10

[Click here to download Non-Rendered Figure: figure10_revised.eps](#)

Figure 11

[Click here to download Non-Rendered Figure: figure11_revised.eps](#)